Published in final edited form as:
DNA Repair (Amst). 2015 February ; 26: 30–43. doi:10.1016/j.dnarep.2014.12.001.

Biochemical characterization of RecA variants that contribute to extreme resistance to ionizing radiation

Joseph R. Piechura[1], **Tzu-Ling Tseng**[2], **Hsin-Fang Hsu**[2], **Rose T. Byrne**[1], **Tricia A. Windgassen**[3], **Sindhu Chitteni-Pattu**[1], **John R. Battista**[4], **Hung-Wen Li**[2], and **Michael M. Cox**[1,*]

[1]Department of Biochemistry, University of Wisconsin – Madison, Madison, Wisconsin 53706-1544

[2]Department of Chemistry, National Taiwan University, Taiwan

[3]Department of Biomolecular Chemistry, University of Wisconsin – Madison, Madison, Wisconsin 53706

[4]Department of Biological Sciences, Louisiana State University and A & M College, Baton Rouge, LA 70803

Abstract

Among strains of *Escherichia coli* that have evolved to survive extreme exposure to ionizing radiation, mutations in the *recA* gene are prominent and contribute substantially to the acquired phenotype. Changes at amino acid residue 276, D276A and D276N, occur repeatedly and in separate evolved populations. RecA D276A and RecA D276N exhibit unique adaptations to an environment that can require the repair of hundreds of double strand breaks. These two RecA protein variants (a) exhibit a faster rate of filament nucleation on DNA, as well as a slower extension under at least some conditions, leading potentially to a distribution of the protein among a higher number of shorter filaments, (b) promote DNA strand exchange more efficiently in the context of a shorter filament, and (c) are markedly less inhibited by ADP. These adaptations potentially allow RecA protein to address larger numbers of double strand DNA breaks in an environment where ADP concentrations are higher due to a compromised cellular metabolism.

1. Introduction

Ionizing radiation (IR) is present in the environment in the form of low levels of X-rays and radionuclides. Higher-level doses may be encountered in the form of X-ray devices and radioactive compounds. However, few organisms are normally exposed to substantial IR

*Address of corresponding author: cox@biochem.wisc.edu.

The authors declare that they have no competing interests.

doses in the environment. Nevertheless, a number of organisms can survive extraordinary exposure to IR, exposure to which damages all cellular components and introduces genomic double strand breaks. The molecular basis of this resistance is of interest due to the potential for human genomic and cellular damage due to IR exposure related to human activities.

The most studied model system for extreme resistance to IR is the bacterium *Deinococcus radiodurans* [1–4]. Whereas a 2–5 Gy dose of IR is lethal for a human, *Deinococcus radiodurans* can survive doses in excess of 5,000 Gy with no lethality [1–5]. The extraordinary resistance of *Deinococcus* to ionizing radiation is likely to be a byproduct of an evolved capacity to withstand long-term desiccation [6, 7].

On the surface, *Deinococcus* appears to possess an unremarkable complement of DNA repair systems. These include recombinational DNA repair (RecA, RecF, RecO, RecR, RecX, RecN, RadA, RuvA, RuvB, RuvC, RecG, RecJ, RecQ, SbcCD), nucleotide excision repair (UvrA, UvrB, UvrC, UvrD), base excision repair (Xth, AP endonuclease, two AlkA glycosylases, nine DNA glycosylases), and mismatch repair (MutS (2 homologs), MutL, UvrD, no NutH homolog) [4, 8]. A handful of novel proteins are present, induced to high levels when Deinococcus is exposed to IR (DdrA, DdrB, DdrC, DdrD, PprA [2, 9], and play a demonstrated role in genome reconstitution. However, the activities of at least some of these proteins suggest a role in genome preservation (perhaps in the context of long term desiccation) rather than a role in a novel DNA repair system [10–13]. The apparent absence of novel DNA repair functions in *Deinococcus* has contributed to arguments that the molecular basis of extreme IR resistance lies in the capacity of the cells to protect its proteins from oxidative damage, rather than any special facility for DNA repair [3, 14, 15].

Deinococcus does appear to utilize its DNA repair functions in a somewhat unusual two-stage process for genome reconstitution, dubbed extended synthesis-dependent single strand annealing, or ESDSA [16–18]. The RecA protein of *Deinococcus radiodurans* (DrRecA) also possesses some novel attributes that might be linked to its function in the context of the reconstitution of an IR-fractured genome. First, under at least some conditions, the DrRecA protein promotes DNA strand exchange with a preferred DNA substrate order of addition that is opposite of that seen with the *E. coli* RecA protein (EcRecA) [19]. Rather than binding single strand DNA first, DrRecA preferentially initiates strand exchange from the duplex DNA substrate [19]. The properties of DrRecA with respect to filament formation are also distinct. The EcRecA protein nucleates filament formation relatively slowly, and extends the filaments more rapidly, properties that would tend to localize much of the available RecA protein in a single filament. This may reflect a repair system that typically must deal with one or only a few situations requiring recombinational DNA repair in each cell cycle. In contrast, the DrRecA protein nucleates more rapidly and extends the filament more slowly, properties which would tend to create large numbers of shorter filaments [20]. These properties are consistent with a system that must deal with hundreds of double strand breaks after desiccation or extreme doses of ionizing radiation.

To better understand the genetic innovations that produce extreme resistance to IR, we have subjected *Escherichia coli* to directed evolution. We have generated strains of *E. coli* that are nearly as resistant to IR as is Deinococcus [21, 22], exhibiting increases in survival of 3–

4 orders of magnitude when exposed to an IR dose of 3,000 Gy. For one of these strains, an isolate called CB2000, we have attributed nearly the entire phenotype to mutations in the genes *recA*, *dnaB*, and *yfjK* [22]. All three mutations reflect broader patterns in the four evolved populations [22]. The overall result demonstrates that adaptation of existing DNA repair systems, rather than evolution of novel repair processes, can make significant contributions to an extreme IR resistance phenotype [22].

In the evolution trials, mutations in the *recA* gene appear prominently in three of four separately evolved populations, and alterations at residue 276 (D276A and D276N) predominate. The D276A RecA mutation makes a substantial contribution to the overall IR resistance phenotype in CB2000 [22]. The RecA alterations, along with other mutations, demonstrate that new DNA repair systems may not be necessary for extreme IR resistance; existing systems can adapt to the new cellular requirements. In spite of over three decades of investigation of the structure and function of RecA protein, the two RecA variants at residue 276 have never been isolated or characterized. The obvious question becomes: what alterations in the molecular repertoire of the RecA protein might contribute to resistance to ionizing radiation? In this report, we investigate the changes in wild type RecA protein function that result from the D276A and D276N mutations, revealing acquired properties that fit the context of repair of a severely degraded genome.

2. Materials and Methods

DNA Substrates

Circular single-stranded DNA and supercoiled double-stranded DNA were obtained from bacteriophage M13mp18 using CsCl gradients as described previously [23–25]. Linear double-stranded DNA for strand exchange reactions was generated by digestion of supercoiled DNA with the restriction enzyme PstI according to the manufacturers instructions. Concentration of DNA substrates was determined using absorbance at 260 nm and the conversion factors 108 μM A_{260}^{-1} for single-stranded DNA and 151 μM A_{260}^{-1} for double-stranded DNA. DNA concentrations in this work are given in total nucleotides.

Cloning and Strain Construction

Construction of pEAW416. *E. coli* radiation resistant evolved strain CB1013 [21, 22] was used as a PCR template with an upstream primer consisting of an NdeI site followed by bases 4–16 of the *recA* gene. The ATG bases of the NdeI site code for the start codon of *recA*. The downstream PCR primer consisted of a BamHI site followed by the last 28 bases of the recA gene. The PCR product was digested with NdeI and BamHI and inserted into the overproduction vector pET21A (Novagen) digested with the same enzymes. The presence of recA D276A was confirmed by direct sequencing. Construction of pEAW446. This was carried out in a similar manner as pEAW416, with E. coli radiation resistant evolved strain CB2000 used as PCR template. The resulting plasmid had *recA* N5K+D276N mutations. The N5K mutation was replaced by a wt N5, and the presence of *recA* D276N was confirmed by direct sequencing.

Protein Purification

Native wild type *E. coli* RecA and single-stranded DNA binding protein were purified as described previously [26]. Protein concentrations were determined using absorbance at 280 nm and the extinction coefficients $2.23 \times 10^4\ M^{-1}\ cm^{-1}$ for RecA [27] and $2.83 \times 10^4\ M^{-1}\ cm^{-1}$ for SSB [28].

E. coli K12 strain STL2669 (Δ(*recA-srlR)306:Tn10xonA2(sbcB*$^-$)), a nuclease-deficient strain which was graciously provided by Susan T. Lovett (Brandeis University), was transformed with pT7pol26 and either pEAW416, encoding RecA D276A, or pEAW 446, encoding RecA D276N [29]. Four liters of Luria-Bertini media supplemented with 100 μg/mL ampicillin and 40 μg/mL kanamycin were inoculated with the appropriate strain and incubated at 37° C with shaking. When the cultures were at an $A_{600\ nm}$ of approximately 0.65, protein expression was induced by the addition of isopropyl 1-thio-p-D-galactopyranoside to a final concentration of 0.4 mM. The cells were allowed to grow for 3 more hours at 37° C with shaking and then were collected by centrifugation. Cell pellets were flash-frozen in liquid N_2 and then adjusted to a concentration of 20 % (w/v) in a solution of 250 mM Tris-HCl (80% cation, pH 7.7) and 25 % (w/v) sucrose and allowed to thaw at 4° C overnight. All subsequent purification steps were carried out at 4° C. Lysis of the cells containing RecA D276N was initiated by the addition of lysozyme to a final concentration of 2.5 mg/mL. EDTA was added to both cell solutions to a final concentration of 7 mM, and cells were lysed by sonication. Cell debris was removed by centrifugation, and RecA protein was precipitated by the addition of 0.111 mL of 5 % (w/v) polyethyleneimine per mL of lysate. The precipitate was pelleted by centrifugation, washed with R buffer (20 mM Tris-HCl (80% cation, pH 7.7), 10% glycerol, 0.1 mM EDTA, 1 mM DTT) for the RecA D276N pellet or R + 100 mM ammonium sulfate for the RecA D276A pellet. Then, protein was extracted from the pellet with R buffer + 300 mM ammonium sulfate. RecA was then precipitated by the addition of ammonium sulfate to a final concentration of 0.28 g/mL The precipitate was pelleted by centrifugation and washed with R buffer + 0.28 g/mL ammonium sulfate. RecA was then resuspended and dialyzed into R buffer + 100 mM KCl. RecA D276A was further purified using successive Q-sepharose, SP-sepharose, and Sephacryl S-300 gel filtration chromatography steps. RecA D276N was further purified using successive DEAE-sepharose, ceramic hydroxyapatite, Source 15-Q, and Sephacryl S-300 gel filtration chromatography steps. The proteins were determined to be >95% pure as determined by SDS-PAGE, dialyzed into R buffer, flash-frozen in liquid N_2, and stored at −80 ° C. RecA proteins were determined to be free of detectable nuclease activity. The concentrations of RecA D276A and RecA D276N were determined using the wild type RecA protein extinction coefficient.

ATP Hydrolysis (ATPase) Assay

A coupled spectrophotometric enzyme assay [30, 31] was employed to measure the rate of ATP hydrolysis of RecA. ADP formed by ATP hydrolysis was converted back to ATP by an ATP regenerationg system of 10 units/mL of pyruvate kinase and 3.5 mM phosphoenolpyruvate. Pyruvate produced by the regeneration reaction was then utilized by a coupling system of 10 units/mL of lactate dehydrogenase and 1.5 mM NADH to oxidize NADH to NAD+. The conversion of NADH to NAD+ was monitored using absorbance at

380 nm, and the extinction coefficient of $\varepsilon_{380} = 1.21 mM^{-1} cm^{-1}$ was used to convert absorbance to amount of ATP hydrolyzed, assuming a stoichiometry of one NADH molecule oxidized per ATP molecule hydrolyzed. Reactions were carried out at 37° C in buffer containing 25 mM Tris-OAc (80% cation), 10 mM magnesium acetate, 3 mM potassium glutamate, 1 mM DTT, and 5 % (w/v) glycerol. The final pH was 7.3. These assays were carried out in a Perkin Elmer Lambda 650 UV/Vis spectrometer equipped with a temperature controller and a 9-position cell changer. Cell path length was 1.0 cm and bandpass was 2 nm. All ATPase assays but the strand exchange reactions not involving the addition of ADP were carried out in this spectrophotometer with the same cuvettes. 5 μM M13mp18 circular ssDNA was incubated for 10 minutes with either 3 μM RecA or 0.5 μM SSB and 3 mM ATP, and then ATP hydrolysis was initiated by the addition of 0.5 μM SSB and 3 mM ATP or 3 μM RecA to the reactions, respectively.

DNA Strand Exchange Reactions

DNA strand exchange reactions were carried out at 37° C in the same buffer used for ATPase assays. The basic reaction scheme involved incubation of RecA with M13mp18 circular ssDNA for 10 minutes. Next, ATP and SSB were added to the reaction and incubated for 10 minutes. DNA strand exchange was then initiated with the addition of homologous M13mp18 linear dsDNA. Exact concentrations are delineated in figure legends. Ten μL time points were removed and deproteinized by addition of 2 μL of 10% (w/v) SDS and 3 μL of 15% (w/v) Ficoll and 20 mM Tris-OAc (80% cation, pH 7.8). Time points were then resolved on a 0.8 % (w/v) agarose gel and visualized with ethidium bromide staining and exposure to UV light. Gel images were captured using a Fotodyne FOTO/Analyst® CCD camera, PC Image acquisition software, and a FOTO/Convertible dual transilluminator. Images were inverted using PC Image software and then DNA band intensity was quantified using TotalLab version TL100 software from Nonlinear Dynamics. Product and intermediate amounts are expressed as a percentage of the total intensity of linear dsDNA, intermediates, and nicked circular product DNA in the respective lane. If ADP was not added to reactions, an ATP regeneration system of 3 mM phosphoenolpyruvate and 10 units/mL of pyruvate kinase was included. Strand exchange reactions in which ATP hydrolysis was measured and ADP was not added contained an ATP regeneration system of 4 mM phosphoenolpyruvate and 10 units/mL of pyruvate kinase and a coupling system of 4.5 mM NADH and 10 units/mL of lactate dehydrogenase. These reactions were carried out in a Varian Cary 300 dual beam spectrophotometer equipped with a temperature controller and a 12-position cell changer. Cell path length was 0.5 cm and bandpass was 2 nm. ATP hydrolysis was followed using absorbance at 380 nm as described above. Strand exchange reactions involving the addition of ADP were normalized by converting the percentage of nicked circular product DNA produced in a given reaction to the percentage of the amount of product formed in the reaction in which no ADP was added. These values were then fit to a dose response (inhibition) curve with variable slope in Prism software to determine IC50 values.

ATPase Assays involving the addition of ADP

As the NADH-based coupling system for ATPase assays described above relies on the regeneration of ADP to produce a signal, the Enzcheck® Phosphate Assay Kit from

Molecular Probes was employed to measure the ATPase activity of RecA when ADP was added to reactions. As inorganic phosphate is released from RecA after an ATP hydrolysis event, the coupling enzyme purine nucleoside phosphorylase utilizes the phosphate ion to convert 2-amino-6-mercapto-7-methyl purine riboside (MESG) to ribose 1-phosphate and 2-amino-6-mercapto-7-methylpurine, which absorbs strongly at 360 nm. Assays were conducted at 37° C in the same buffer used for the NADH-based ATPase assays and contained 0.2 mM MESG and 1 unit/μL of purine nucleoside phosphorylase. First, 1 μM M13mp18 circular ssDNA was incubated with 0.6 μM RecA protein for 10 minutes. Then, ATP hydrolysis was initiated by the addition of 1 mM ATP and 0.1 μM SSB. ADP was then added five minutes after the addition of ATP. If strand exchange reactions were carried out, 2 μM M13mp18 linear dsDNA was added at the same time as ADP. Absorbance was measured at 360 nm during the reaction in a Perkin Elmer Lambda 650 UV/Vis spectrometer as was used for the NADH-based assays. A standard phosphate curve was generated in order to convert absorbance at 360 nm to the concentration of phosphate generated by ATP hydrolysis. Briefly, varying amounts of phosphate were added to reaction buffer containing the coupling system and incubated at 37° C until aborbance readings at 360 nm were constant. A linear fit line was applied to the linear portion of the graph of phosphate concentration vs. A_{360} . This analysis generated a conversion factor of 0.0132 A_{360} Pi^{-1} (μM), and revealed that the coupling system produced a linear signal up to a concentration of approximately 100 μM Pi.

Data was further analyzed in the program CurveExpert. If no ADP was added to reactions, the rate of ATP hydrolysis was determined by applying a linear fit to the data. If ADP was added, a polynomial fit (n=6) was applied to the data and differentiated at time 7 minutes after the addition of ADP. Data from three independent experiments was averaged and these values were converted to the percentage of the uninhibited rate of ATP hydrolysis. Standard deviation values were determined using standard statistical methods.

Single-molecule experiments

For real-time RecA nucleoprotein assembly observations at the single-molecule level, experimental details are the same as previously described [20]. Duplex DNA with a length of 382 bp was prepared by polymerase chain reaction (PCR) using a 5′-digoxigenin-labeled primer (5′-dig-ACTACGATACGGGAGGGC), a 5′-biotin-labeled primer (5′-biotin-TGAGTGATAACACTGCGGC) and pBR322 templates. PCR products were gel purified (Qiagen). Individual dsDNA molecules were tethered on the antidigoxigenin-coated slide, and the distal end of the DNA molecules were attached to streptavidin-labeled beads for visualization under optical microscope. Individual tethered DNA molecules were screened and verified as single DNA tethers by both the BM amplitude of the 382 bp DNA and the symmetric BM trajectory (x/y ratio ~ 1). To observe the RecA nucleoprotein assembly process, a 40 μL mixture of RecA (2 μM) with ATP (2 mM, Aldrich), 10 units/mL pyruvate kinase (Roche) and 3 mM phosphoenolpyruvate (Aldrich) in the single-molecule buffer (25 mM MES, pH 6.20, 10 mM magnesium acetate, 3 mM potassium glutamate, 1 mM dithiothreitol, 5 % glycerol, and 1 mg/mL BSA) was flowed into the reaction chamber. All reactions were conducted in 22°C. Flow deadtime is 10 s.

Electron Microscopy

A modified Alcian method was used to visualize RecA nucleoprotein filaments. Activated grids were prepared as described previously [32]. Samples for electron microscopy analysis were prepared as follows. All incubations were carried out at 37 °C. Reactions contained 6 μM M13mp8 circular ssDNA, 25 mM Tris-OAc (80% cation) buffer, 5% (w/v) glycerol, 3 mM potassium glutamate, and 10 mM Mg $(OAc)_2$, and an ATP regeneration system of 10 units/ml creatine kinase and 12 mM phosphocreatine. These components were incubated along with 3mM ATP and 1.0 μM SSB for 10 min. RecA or RecA variant proteins (to 3 μM), or the equivalent volume storage buffer, was added and incubation continued for another 5 min. ATPγS was then added to a final concentration of 5 μM. Samples were spread immediately. The reaction solution was diluted to a final DNA concentration of 0.0004 μg/μl with 200 mM ammonium acetate, 10 mM HEPES (pH 7.5) and 10% glycerol and adsorbed onto the Alcian grids for 3 min. The grids were then touched to a drop of the above buffer, followed by floating on a drop of the same buffer for 1 min. The sample was then stained by touching to a drop of 5% uranyl acetate followed by floating on a fresh drop of 5% uranyl acetate for 30 s. Finally, the grid was washed by touching to a drop of double distilled water followed by immersion in two 10-ml beakers of double distilled water. After the sample was dried, it was rotary-shadowed with platinum. This protocol is designed for visualization of complete reaction mixtures, and no attempt was made to remove unreacted material. Although this approach should yield results that provide insight into reaction components, it does lead to samples with a high background of unreacted proteins.

A RecA filament was considered gapped, if the ssDNA molecule to which it was bound had a detectable region of SSB-coated DNA of any size. Visual judgments were used to place individual RecA filaments in five categories: large, medium, small or very small filamented circles (very small filamens are molecules with very short RecA filaments and the rest of the molecule coated with SSB) or SSB/DNA molecules. For each RecA variant, length measurements were carried out using Metamorph analysis software on molecules selected at random from each of the five categories above that represented more than 10% of the total molecules in a given sample. The complete set of measurements is provided in Table S1. Each filament was measured three times, and the average length was calculated. The 500 μm scale bar was used as a standard to calculate the number of pixels per μm. Each nucleoprotein fragment length, originally measured by Metamorph in pixels, was thus converted to μm.

Filaments with large filamented circles had filaments averaging 3.23 +/− 0.29 μm in length. This category generally included filaments that were full length or nearly so, and ranged from 3.03 to 3.6 μm. Filaments with medium filamented circles averaged 2.32 μm in length, with a range of 1.73 to 2.72 μm. Small filamented circles averaged 1.28 μm, with a range of 0.97 to 1.8 μm. Molecules judged to have very small filaments had RecA filaments averaging 0.39 μm in length, with a range of 0.12 to 0.71. Linearized DNA molecules originating likely from shearing force during pipetting were also counted. With the total number of filaments counted as 100%, the percentage of each type of nucleoprotein filament was calculated. To determine the proportion of the molecules observed that were either fully or partially coated by RecA protein or bound only by the SSB protein, at least two separate

regions of two separate grids, from two independent sets of experiment or four grids (encompassing at least 2000 DNA molecules) were counted at the identical magnification for each sample.

Imaging and photography were carried out with a TECNAI G2 12 Twin Electron Microscope (FEI Co.) equipped with a GATAN 890 CCD camera. Digital images of the nucleoprotein filaments were taken at X 15000 Magnification.

3. Results

3.1 RecA D276A and RecA D276N hydrolyze ATP moderately faster than Wild type RecA when bound to circular ssDNA and more readily displace SSB from circular ssDNA

We began our investigation of the RecA D276A and RecA D276N proteins with an analysis of ATPase activity on circular single-standed DNA (circular ssDNA). Excess RecA protein or RecA protein variant was added to circular ssDNA to allow the protein to bind and filament on the DNA. ATP was then added to initiate ATP hydrolysis. SSB was added with ATP to remove secondary structure from the circular ssDNA and allow for formation of contiguous RecA filaments. RecA was present in excess of ssDNA, and the 3 mM ATP added was approximately 150 fold greater than the measured K_m for wild type RecA protein bound to ssDNA [33]. ATPase activity is thus reported here as apparent k_{cat}, calculated by dividing the observed rate of ATP hydrolysis by the number of RecA binding sites in solution (the ssDNA concentration in total nucleotides divided by 3). Wild type RecA hydrolyzed ATP with an apparent k_{cat} of 29.3 ± 0.8 min^{-1}, which agrees well with the literature value of 30 min^{-1} [34–39]. As shown in Figure 1, RecA D276A and RecA D276N displayed a small but significant increase in the rate of ATP hydrolysis compared to wild type RecA, with apparent k_{cat} values of 32.8 ± 0.6 min^{-1} and 33.1 ±0.9 min^{-1}, respectively.

The capacity of the RecA variants to displace SSB protein from DNA was examined next (Figure 1). In these experiments, ATP and SSB were added to circular ssDNA first to allow SSB to bind and coat the circular ssDNA, and then RecA protein was added to initiate ATP hydrolysis. A long lag was observed before a steady state rate of ATP hydrolysis was reached for all proteins, consistent with the fact that RecA protein has a quite limited capacity to displace SSB from ssDNA [40–43]. As conditions for ATP hydrolysis were not optimal, k_{cat} was not calculated for these experiments. An apparent lag time was calculated by extrapolating the most linear portion of each curve to the x axis to estimate the time required for the maximum rate observed over a 90 min timecourse to be reached. Wild type RecA hydrolyzed ATP with a maximum observed rate of 22 ± 1 μM/min (compared with the approximately 50 μM/min that would be produced if the ssDNA were saturated by RecA protein). The lag time needed to reach this rate was 36 ± 3 min. Interestingly, RecA D276A hydrolyzed ATP at a maximum rate of 31 ± 2 μM/min with a lag time of 23 ± 3 min and RecA D276N hydrolyzed ATP at a maximum rate of 34 ± 2 μM/min with a lag time of 21.7 ± 0.3 min. This data suggests that RecA D276A and RecA D276N have a somewhat enhanced capacity to displace SSB from DNA, although they do not approach the capacity of classic RecA mutants such as RecA E38K (RecA730) or RecAAC17 [41, 42].

3.2 RecA D276A and RecA D276N hydrolyze ATP faster while catalyzing strand exchange but resolve strand exchange intermediates into products somewhat slower than wild type RecA

Next, the strand exchange activity of the RecA variants was characterized. Contiguous RecA filaments were formed on circular ssDNA as described above and were allowed to hydrolyze ATP for 20 minutes. Then, homologous linear double-stranded DNA (linear dsDNA) was added to initiate strand exchange. RecA filaments on circular ssDNA pair the DNA with homologous DNA in the linear dsDNA and then exchange the circular ssDNA with the identical strand in the linear dsDNA, creating a newly paired nicked circular DNA duplex (Fig. 2A). After addition of linear dsDNA, time points were removed, deproteinized, and resolved on an agarose gel to follow the progression of DNA strand exchange. ATP hydrolysis was also measured and activity is expressed as apparent k_{cat} as described above.

When bound to circular ssDNA, wild type RecA hydrolyzed ATP with an apparent k_{cat} of $27.9 \pm 0.8\ min^{-1}$ in this experiment. This rate is slightly slower than the one reported above, likely due to the potentially inhibitory higher concentration of PEP included in these reactions to extend the lifetime of the ATPase coupling system. Once strand exchange was initiated, the rate of hydrolysis of Wild type RecA decreased by nearly 1/3, to an apparent k_{cat} of $18.7 \pm 0.5\ min^{-1}$. The decline reflects a change in state of the RecA filament that is dependent on the length of homology in the duplex DNA substrate [23, 44]. Consistent with the above results, RecA D276A and RecA D276N hydrolyzed ATP slightly faster than Wild type RecA when bound to circular ssDNA, with apparent k_{cat} values of $30.7 \pm 0.7\ min^{-1}$ and $31.1 \pm 0.4\ min^{-1}$, respectively. Interestingly, the decline in rates of ATP hydrolysis observed upon addition of homologous duplex DNA was much attenuated with RecA D276A and RecA D276N. The RecA variants hydrolyzed ATP much faster than wild type RecA while catalyzing strand exchange, with apparent k_{cat} values of $26.6 \pm 0.6\ min^{-1}$ and $27.7 \pm 0.4\ min^{-1}$, respectively, observed after dsDNA addition. Thus, RecA D276A and RecA D276N hydrolyze ATP faster than wild type RecA when bound to circular ssDNA and when catalyzing strand exchange, but this difference in activity is much more pronounced during DNA strand exchange. This may reflect an incomplete transition to a state in which DNA strand exchange and ATP hydrolysis are coupled for the wild type protein [23].

The agarose gel pictures in figure 2C illustrate the progression of the strand exchange reactions catalyzed by the RecA variants. DNA substrates, reaction intermediates (Int), and the nicked circular duplex product are readily distinguishable and are labeled on the gels. Figure 2D presents a quantification of the reactions, carried out as described in *Experimental Procedures*. Wild type RecA, RecA D276A, and RecA D276N all produced similar amounts of reaction intermediates 5 minutes after the addition of linear dsDNA, suggesting that when RecA is present in excess of circular ssDNA, these proteins display a similar capacity for pairing homologous DNAs. However, product DNA was visible in the reaction promoted by wild type RecA reaction about 5 minutes before it was visible in the RecA D276A and RecA D276N reactions. Furthermore, more product DNA was present at significantly higher levels in the wild type RecA reaction at 10, 15, and 20 minutes after the addition of linear dsDNA. At later time points, all three RecA variants produced similar amounts of product DNA. This data suggests that RecA D276A and RecA D276N show wild type activity in pairing

homologous DNA when RecA protein is present in excess of circular ssDNA, but the resolution of reaction intermediates into product is somewhat impeded in these mutants. A demonstrable coupling of ATP hydrolysis and DNA strand exchange has been documented in earlier studies [39, 45–47]. Together, the reduced decline in ATP hydrolysis triggered by dsDNA addition, and the slower resolution of intermediates to products, may signal a relaxation of this coupling for these variant RecA proteins. In all of the activities examined in Figures 1 and 2, the effects are relatively small but readily measurable.

The reduced decline in ATP hydrolysis upon addition of dsDNA does not reflect a reduced dependence of the ATPase activity on DNA binding. In the absence of DNA, no notable ATPase activity was detected for either mutant protein. For example, the apparent $k_{cat} = 0$, 0.4, and 0 min^{-1} for the wild type, D276A, and D276N proteins, respectively, in one trial.

3.3 RecA protein filament extension on dsDNA is slowed by the D276 mutations

The relatively slow nucleation of wild type *E. coli* RecA protein on DNA, coupled with more rapid filament extension [20, 48–51], would tend to create small numbers of long RecA protein filaments in the cell. This would be appropriate in an unstressed *E. coli* cell dealing with no more than one or two DNA lesions requiring recombinational DNA repair in a cell cycle [52, 53]. We have recently made use of single-molecule tethered particle motion (TPM) experiments to study the assembly dynamics of *E. coli* and *D. radiodurans* RecA proteins on individual duplex DNA molecules by observing changes in dsDNA tether length and stiffness resulting from RecA binding [20]. Relative to the *E. coli* RecA, DrRecA protein filaments nucleate more rapidly and extend more slowly [20], parameters that would tend to create more numerous and shorter filaments. We applied the TPM technology to examine the kinetic parameters of RecA filament formation with the RecA D276 variants. The DrRecA protein was included in this set of experiments to provide a comparison with a RecA that is adapted to IR resistance. These experiments allow us to examine rates of nucleation and extension directly. However, of necessity, these experiments are done with duplex DNA and at room temperatures. Parts of the work are extrapolated to single-stranded DNA and 37 °C in the section that follows.

We immobilized one end of a 382 bp dsDNA segment on a surface and attached the other end to a bead. The approach takes advantage of the properties of RecA, in which binding to dsDNA leads to a 1.5 fold increase in length and an increase in filament stiffness [54, 55]. This in turn leads to a measurable change in the bead's Brownian motion (BM). The method of tethered particle motion (TPM) has been widely used in single-molecule studies, addressing problems such as the size of a loop formed by a repressor [56], the folding and unfolding state of G-quadruplex[57], and translocation on DNA by polymerases [58] and RecBCD helicase/nuclease [59]. When applied to RecA filament formation, changes in the length and rigidity of the DNA tether that occur upon RecA binding result in an increase in the spatial extent of bead BM. This change of bead motion can be measured to nanometer precision using digital image processing techniques that determine the standard deviation of the bead centroid position in light microscope recordings [57, 59–61].

Typical time-courses of RecA protein assembly on a 382 bp duplex DNA are shown in the left column of Figure 3. After a 1,000-frames (33 s) recording of the BM of dsDNA tethers,

a mixture of RecA protein and ATP was introduced in the reaction chamber at the time indicated with a grey bar, with a deadtime of about 10 seconds due to focus re-stabilization. The same DNA tether was recorded to monitor the RecA assembly process. In all cases, the DNA tether length stayed constant until reaching a point where an obvious, continuous increase in BM was observed. The DNA tether length then stayed constant at the higher BM amplitude, consistent with the BM value we measured separately for fully coated RecA-dsDNA filaments (data not shown).

We define the dwell time between the RecA introduction and the time where apparent BM change occurred as the nucleation time, the continuous BM increase region as the DNA extension caused by RecA assembly (the rate calculated from the slope), and the high BM value where DNA tether length stayed constant as the maximum BM achieved [20]. Experiments and analysis were first done with wild type RecA. We then applied this method to study the RecA protein variants. The Deinococcus RecA protein (DrRecA) was included in the experiments to provide an interesting point of reference. The nucleation of all of these RecA proteins onto dsDNA is highly pH-dependent [62, 63]. To permit reasonably convenient observation in real time, these reactions were carried out at pHs below neutrality.

The results are summarized in Figure 3A. The more rapid nucleation of the DrRecA protein, relative to wild type EcRecA, is seen in the first column of binned results. The average nucleation time (τ) is 51 seconds for DrRecA relative to 449s for EcRecA. A reduction in nucleation time to 146 seconds is also seen for the RecA D276A mutant protein. However, this is not a general pattern, as seen by the increase in τ seen for D276N RecA protein to 841 seconds. A consistent pattern is observed when the rate of filament extension is considered (the second column of binned results). The average rate of filament extension for wild type EcRecA protein is indicated by the vertical dashed line. For DrRecA, the average extension rate is slower, as shown by the leftward shift in the profile of Figure 3. A very similar leftward shift to slower filament extension rates is seen in the second column of binned results for both of the RecA D276 variants. We note that the maximum Brownian motion seen with those same D276 variants is identical to that seen with wild type EcRecA protein, as shown in final column of binned results in Figure 3A. Thus, both RecA D276 variants exhibit slower filament extension rates that could lead to the formation of shorter RecA protein filaments on DNA, at least under these experimental conditions.

In Figure 3B, we examine the pH-rate profiles for the nucleation of filament formation for all of the RecA proteins examined here. Although the data is limited to pHs between 6 and 6.5, a clear dependence of nucleation rates on pH is seen that is consistent with the dependence observed in earlier studies [63]. We note that the slope of the best-fit lines, obtained for this limited data set, is somewhat steeper for the wild type RecA protein than is seen for the D276 variants. Although more work is required, this may suggest that ionization of D276 plays a direct role in the nucleation process in the wild type protein.

3.4 More rapid nucleation of the RecA D276A and D276N variants can be observed by electron microscopy at physiological pH and temperature

Of necessity, the single molecule experiments must be carried out at room temperature and at lower pHs where the measurements can be completed in a reasonable timeframe. To

extend these observations to the higher pH (7.3) and temperature (37°C) utilized for the ATPase and strand exchange experiments, and to single-stranded DNA, we examined filament formation by electron microscopy. M13mp18 ssDNA circles were first bound with SSB. RecA protein was added and reactions were halted and spread after 5 min as described in Methods. Molecules with visible RecA filaments were binned into four categories, reflecting the lengths of coated DNA. These ranged from very short filaments, small circles, medium circles, and large circles. Single stranded DNAs coated only with SSB were counted as a fifth category. The large circles reflect complete or nearly complete RecA filamentation on that molecule. Measurements of a subset of the filaments in each category are presented in Table S1.

As shown in Figure 4, the fraction of DNA molecules with RecA filaments was substantially higher for the two RecA protein variants. Most of the DNA in the sample utilizing wild type RecA protein remains as SSB-coated circles, one of which is highlighted in panel B. This result implies a significant increase in nucleation rate on SSB-coated ssDNA in this experiment for the D276A and D276N mutant proteins. The D276 mutant proteins also exhibited filaments that extended over longer regions of the ssDNA. However, breaks in the filaments – either obvious breaks that included visible bound SSB or sharp bends in the RecA filament that suggested discontinuities (highlighted in Fig. 4, panel C) – were common. Ambiguity about the number of nucleation events represented in each filament make it impossible to make conclusions about relative filament extension rate.

3.5 RecA D276A and RecA D276N more efficiently catalyze strand exchange when present at sub-saturating levels relative to the circular ssDNA substrate

To better characterize the strand exchange activity of RecA D276A and RecA D276N, a series of strand exchange reactions were carried out to examine reaction efficiency as a function of RecA protein concentration. As a RecA monomer binds 3 nucleotides [54, 64–66], 100%, 75%, 50%, 33%, 20%, and 10% saturation of 10 μM M13mp18 circular ssDNA were defined as 3.33 μM, 2.50 μM, 1.67 μM, 1.10 μM, 0.67 μM, and 0.33 μM RecA. RecA protein was allowed to incubate with circular ssDNA for 10 minutes, 3 mM ATP and 1 μM SSB were added and incubated with RecA for 10 minutes, and then 20 μM M13mp18 linear dsDNA were added to initiate the reaction. The reactions were allowed to proceed for 90 minutes before being deproteinized and resolved on a gel for quantification.

At 100% and 75% saturation, all three RecA proteins produced similar amounts of strand exchange products (Figure 5A). Interestingly, at lower RecA protein concentrations, RecA D276A and RecA D276N consistently produced more strand exchange products than wild type RecA in three independent experiments (Figure 5A). The difference is most striking at 10% saturation, where RecA D276A and RecA D276N produce approximately 3 fold more product than wild type RecA. As saturation increases, the fold difference between wild type RecA and the mutants becomes smaller, but remains significant until 75% saturation. RecA D276A and RecA D276N exhibited essentially identical levels of activity in this assay, generating the same amount of product within error at all levels of saturation. Most important, the RecA D276 variants generated substantially higher levels of product than

wild type RecA protein at subsaturating RecA protein concentrations. The results suggest that the mutant proteins function better when present as short filaments.

To explore the mechanism of this difference in catalytic activity, a time course strand exchange reaction was carried out with RecA present at 1.1 μM, or 33% saturation of the available circular ssDNA. The results from three separate experiments are quantified in Figure 5B. Consistent with the previous experiments, RecA D276A and RecA D276N produced approximately 1.65 fold more product than wild type RecA after the reactions had proceeded for 90 minutes. Even though the final yield of products was higher, RecA D276A and RecA D276N catalyzed the resolution of strand exchange intermediates into product DNA occurred somewhat more slowly than wild type RecA, as seen in Figure 2. The yield advantage was nevertheless evident at all stages of the reaction. At 20 minutes after the addition of linear dsDNA, RecA D276A and RecA D276N produced 1.85 fold more intermediates than wild type RecA. Furthermore, these intermediates are not present at high levels at times outside of the times when intermediates are at maximum levels in the normal wild type reaction, as might be expected if RecA D276A and RecA D276N were increasing yield by promoting multiple rounds of strand exchange. Thus, the data presented above supports the hypothesis that RecA D276A and RecA D276N more efficiently catalyze the pairing of homologous DNA strands when RecA is present at sub-saturating levels of circular ssDNA.

3.6 The DNA strand exchange activity of RecA D276A and RecA D276N is much less inhibited by ADP

An underappreciated property of the wild type RecA protein is its sensitivity to inhibition by ADP. If no ATP regeneration system is included in the reaction, and ADP levels are allowed to rise, the RecA filaments will disassemble entirely as the ADP/ATP ratio approaches 1.0 [67–69]. Effective DNA strand exchange will halt well before that point. Under normal logarithmic growth conditions, ADP is rarely present at levels sufficient to affect RecA function [70]. However, heavy irradiation of cells has the potential to compromise metabolic processes, leading to unpredictable alterations in the available nucleotide pools. ADP inhibition of RecA protein has the potential to be a significant barrier to recombinational DNA repair under these circumstances.

We examined the effects of ADP on our D276 variant RecA proteins. Strand exchange reactions were carried out without an ATP regeneration system, and were initiated in the presence of varying levels of ADP. First, 2 μM RecA was incubated with 5 μM M13mp18 circular ssDNA for 10 minutes. Next, 5 mM ATP and 0.5 μM SSB were added and incubated for 10 minutes to allow formation of contiguous RecA filaments. Then, 10 μM M13mp18 linear dsDNA and 0, 1, 2, 3, 4, or 5 mM ADP were added to initiate strand exchange. Strand exchange reactions were allowed to proceed for 60 minutes before being deproteinized and resolved on a gel for quantification.

If no ADP was added with linear dsDNA, wild type RecA converted 48% of the DNA substrates to nicked circular product (Figure 5). As the concentration of ADP added increased, the amount of product produced by wild type RecA decreased rapidly (Figure 6). The strand exchange activity of wild type RecA was completely inhibited by the addition of

4 mM ADP to the reaction, with trace amounts of activity seen when 3 mM ADP was added (Figure 6). Strikingly, RecA D276A and RecA D276N produced considerably more product than wildtype RecA at all ADP concentrations (Figure 6). This difference in activity was most striking when 2 mM ADP was added to the reactions, as RecA D276A and RecA D276N produced approximately 6 times more product than wild type RecA. The strand exchange activity of RecA D276A and RecA D276N was completely inhibited by the addition of 5 mM ADP, with trace amounts of activity seen when 4 mM ADP was added to the reactions (Figure 6). This data provides clear evidence that the DNA strand exchange activity of RecA D276A and RecA D276N is much less inhibited by ADP than the activity of wild type RecA.

3.7 The ATPase activity of RecA D276A and RecA D276N during strand exchange is less inhibited by ADP than that of Wild type RecA

Next, the effect of ADP on the ATP hydrolysis activity of RecA D276A and RecA D276N during strand exchange was examined. RecA protein was allowed to hydrolyze ATP while bound to circular ssDNA for five minutes, and then homologous linear dsDNA and varying concentrations of ADP were added. ATP hydrolysis was monitored in real time using a method that does not rely on ATP regeneration (see Experimental Procedures). DNA and protein concentrations were reduced 3–5 fold from the strand exchange reactions described above to allow for measurable steady state rates of ATP hydrolysis, but the same ratios of RecA:ATP:ADP were employed in these assays. ADP was again added at the same time as the linear duplex DNA was added to initiate the reaction.

When linear dsDNA but no ADP was added to filaments of Wild type RecA, a steady state rate of ATP hydrolysis was observed (Figure 7A). However, as the concentration of ADP added was increased, an increasingly abrupt drop in the rate of ATP hydrolysis was observed (Figure 7A). As RecA must be bound to DNA to hydrolyze ATP, this observation suggests that the addition of ADP leads to disassembly of RecA filaments. The apparent extent of filament disassembly caused by the addition of ADP was quantified by determining the instantaneous rate of ATP hydrolysis at the point 7 minutes after the addition of ADP and linear dsDNA, as described in *Experimental Procedures*. These rates were then expressed as the percentage of the rate of the reaction in which no ADP was added (Figure 7B). The decline in the rate of observed rate of ATP hydrolysis at time 7 minutes was quite rapid for the wild type protein (Figure 7B). Only 10 % of the uninhibited rate of hydrolysis remained if 0.9 mM ADP was added, and the level of ATP hydrolysis was essentially negligible at time 7 if 1.5 mM ADP was added (Figure 7B).

The effect of ADP on the ATP hydrolytic reaction promoted by RecA D276A or RecA D276N was much less severe (Figure 7B). Significant ATPase activity remained even when 1.2 mM ADP was included in the reaction.

RecA filaments on single-stranded DNA exist in different states before and after strand exchange is initiated [23, 44]. We thus again examined the effect of ADP on RecA D276A and RecA D276N filaments using the protocol of Figure 6, but in the absence of added linear duplex DNA. As shown in Figures 8A and 8B. the differences in the effects of ADP between the wild type and variant proteins was much reduced when the proteins were not

promoting DNA strand exchange. This was due primarily to a reduction in the inhibitory effects of ADP for the wild type protein in the absence of ongoing strand exchange (compare Figures 7B and 8B). The inhibitory effect of ADP on the RecA D276 mutants was similar in both sets of experiments.

4. Discussion

Upon irradiation to 3,000 Gy, a bacterial cell must deal with hundreds of DNA double strand breaks as well as substantial damage to other cellular components. In principle, the damage could include alterations in metabolic processes that could affect the pool of metabolites, including nucleotides, available for genome reconstitution. Directed evolution produces strains of *E. coli* that can deal with this situation [21, 22], and RecA mutations affecting the Asp residue at position 276 contribute substantially to IR resistance in many of those strains. Our results show that the D276 alterations adapt RecA function to IR exposure in at least three important ways.

First, the mutations increase rates of nucleation and slow the growth of RecA filaments on dsDNA after nucleation, under the conditions utilized here for single-molecule measurements. If these changes also apply to nucleation of RecA on ssDNA, this would lead to the formation of shorter and more numerous RecA filaments in an irradiated cell that possesses numerous ssDNA overhangs resulting from double strand breaks. This would in turn facilitate the formation of RecA filaments at more locations to effect repair of numerous double strand breaks. At 37 °C, we confirmed that RecA filament nucleation was accelerated for the D276A and D276N mutant proteins relative to the wild type on SSB-coated ssDNA, which is a likely repair substrate for RecA in the cellular context.

Second, the RecA D276A/N mutants promote DNA strand exchange more efficiently than the wild type proteins when they are present in sub-saturating amounts relative to the DNA substrates. As the improvement in strand exchange product yield is preceded by a large improvement in the generation of strand exchange intermediates, the advantage of the mutant proteins appears to lie at the initiation of strand exchange. In the context of the *in vitro* strand exchange assay used here, productive strand exchange must be initiated via pairing at the end of the linear duplex DNA substrate, requiring the presence of part of a RecA filament at the specific complementary sequences on the ssDNA. At a particular sub-saturating RecA protein concentration and at a particular moment, the RecA mutants should be no more likely to occupy a particular stretch of DNA than the wild type. The enhanced capacity of the mutant RecA proteins to initiate strand exchange may thus reflect more dynamic filaments that can utilize end-dependent assembly and disassembly processes to more rapidly reposition shorter filaments on the DNA. Alternatively, the mutant proteins may simply promote the initial steps of DNA pairing more efficiently than the wild type protein, making initiation more likely when the filament is properly positioned. A much broader analysis of the properties of these mutants is needed to distinguish between these possibilities.

Third and finally, the mutant proteins are substantially less inhibited by ADP during strand exchange than is the wild type protein. It is difficult to assess all of the effects of ionizing

radiation on cellular functions. In addition, it is likely that those effects would vary from cell to cell depending on which critical macromolecules were randomly inactivated. In principle, the capacity of the cell to generate ATP could be compromised in a number of different ways. Any protein/enzyme inactivation that led to an increase in cellular ADP concentrations would hamper recombinational DNA repair in a wild type *E. coli* cell, since RecA function would be affected. At a minimum, this particular property change in the D276 mutants expands the environmental space in which RecA can operate effectively.

We do not know whether the D276 mutations have any effect on RecA's many interactions with other proteins, such as LexA [71–73], RecX [74–76], DNA polymerase V [77–79], etc. Additional work will be required to determine if any such effects exist, and if they affect the observed contribution of the mutant RecA proteins to IR resistance.

We do not wish to imply that these mutant *E. coli* RecA proteins in any way reprise the function and properties of the RecA protein of *Deinococcus radiodurans*. We have found no evidence for an increased capacity to promote the inverse strand exchange readily promoted by DrRecA [19, 80]. We note that the evolution experiment that yielded the EcRecA protein variants at position 276 required about a month to complete [21, 22]. The DrRecA protein has obviously evolved over a much longer period of time.

In sum, the observed alterations in RecA function brought about the D276 mutations exhibit a molecular logic that appears to conform in a reasonable way to the molecular requirements for genome reconstitution after extreme exposure to ionizing radiation. There may be additional effects of these mutations that will be elucidated by more detailed studies.

The classic RecA E38K (*recA*730) mutant protein shares some properties with the D276 mutants studied here, including an increased capacity to displace SSB and more rapid association with DNA [42]. However, strains expressing RecA E38K protein are more rather than less sensitive to radiation. The key difference may lie in the balance between association and dissociation, in the relative rates of the nucleation and filament extension phases, and in the sensitivity of the proteins to ADP. Clearly, it is not enough simply to bind to DNA faster. The status of the filaments and their capacity to function in a compromised cell are also likely to be important factors.

In the course of this work, we considered several molecular explanations for the effects of the D276 alterations. D276 resides in the C-terminal domain of RecA, a region of the protein that is not involved in DNA or ATP-binding but is observed to make large conformational shifts which could represent a switch from an active and inactive conformation [54, 55, 81]. The carboxyl group of D276 is approximately 20 angstroms from the 2′ hydroxyl of the ribose moeity of the ADP-AlF_4-Mg complex in the X-ray crystal structure of RecA bound to ssDNA [54]. Thus, any effect of mutation in this residue on nucleotide binding must be indirect. D276 resides within the helix closest to the connection between the C-terminal domain and the core domain of RecA, and this helix is connected to a turn that makes direct contacts with the adenine and ribose moieties of the ATP in the active site [54]. Furthermore, D276 forms a salt bridge with K302, which resides within a more distal helix from the core. Thus, it is possible that this salt bridge is responsible for transmitting

conformational shifts from the core nucleotide-binding domain to the C-terminal domain of RecA. Mutating an aspartate to either an alanine or an asparagine would eliminate this salt bridge at neutral pH, and could thus render the RecA D276A and RecA D276N variants less able to shift from a strand exchange proficient conformation with a high affinity for ATP to a strand-exchange inactive conformation with a high affinity for ADP. However, studies of a potentially complementary K302A mutation of RecA protein did not replicate the effects of the D276 mutants in any way (J. Piechura, unpublished data).

Another possible, but not mutually exclusive mechanism for the efficient strand exchange phenotype of RecA D276A and RecA D276N is that these mutations affect DNA pairing. K302 is part of a large cluster of nine positively charged surface residues found between residues 270 and 328 [82]. Within this cluster, K302 is one of two lysines that are particularly well conserved among bacterial RecA proteins. The positively charged cluster has been implicated in having a role in capturing homologous dsDNA for formation of joint molecules [83]. In wild type RecA, the salt bridge D276-K302 would presumably restrict movement of K302 residue and might interfere with DNA-pairing activity. In RecA D276A/D276N, the lack of this salt bridge might allow more freedom for K302 to move in solution and thus aid these proteins in more readily initiating DNA pairing.

In a broader sense, our results speak to the malleability of RecA protein function. While not unique to RecA, this is a feature of the protein that is increasingly evident in comparisons of RecA proteins from different bacteria. The variations are sometimes subtle and sometimes not [19, 84–87]. The same theme is highlighted in recent work demonstrating substantial improvements in the capacity of some mutant variants of *E. coli* RecA protein to promote conjugational recombination [88]. Most important, the variations do not reflect an evolutionary approach to some common and most efficient platform for DNA pairing and strand exchange. Homologous genetic recombination is both a benefit and a potential hazard to every cell. A maximally efficient recombinase is not the ideal for all cells, and possibly not the ideal for any cell. The RecA protein structure, shared by RecA homologs in virtually all organisms, is a highly adaptable scaffold readily tailored by evolution to the requirements for genome maintenance in each particular organism.

Supplementary Material

Refer to Web version on PubMed Central for supplementary material.

Acknowledgements

The authors thank Douglas Weibel and his laboratory for use of the Metamorph software for electron microscopy measurements. We also thank Taejin Kim for carrying out a few ATPase assays on these mutant proteins.

Funding: This work was supported by grant GM32335 from the National Institutes of Health of the United State of America (to MMC) and grant 100–2113-M-002–009-MY2 from the National Science Council of Taiwan (to HL). The authors acknowledge use of instrumentation supported by the UW MRSEC (DMR-1121288) and the UW NSEC (DMR-0832760).

References

1. Blasius M, Hubscher U, Sommer S. *Deinococcus radiodurans:* What belongs to the survival kit? Crit. Rev. Biochem. Mol. Biol. 2008; 43:221–238. [PubMed: 18568848]
2. Cox MM, Battista JR. *Deinococcus radiodurans* - The consummate survivor. Nature Rev. Microbiol. 2005; 3:882–892. [PubMed: 16261171]
3. Daly MJ. Death by protein damage in irradiated cells. DNA Repair. 2012; 11:12–21. [PubMed: 22112864]
4. Slade D, Radman M. Oxidative Stress Resistance in *Deinococcus radiodurans* . Microbiol. Mol. Biol. Rev. 2011; 75:133–191. [PubMed: 21372322]
5. Battista JR. Against all odds - the survival strategies *of Deinococcus* radiodurans. Annu. Rev. Microbiol. 1997; 51:203–224. [PubMed: 9343349]
6. Mattimore V, Battista JR. Radioresistance of *Deinococcus radiodurans:* functions necessary to survive ionizing radiation are also necessary to survive prolonged desiccation. J. Bacteriol. 1996; 178:633–637. [PubMed: 8550493]
7. Rainey FA, Ray K, Ferreira M, Gatz BZ, Nobre MF, Bagaley D, Rash BA, Park MJ, Earl AM, Shank NC, Small AM, Henk MC, Battista JR, Kampfer P, da Costa MS. Extensive diversity of ionizing-radiation-resistant bacteria recovered from Sonoran Desert soil and description of nine new species of the genus *Deinococcus* obtained from a single soil sample. Appl. Environ. Microbiol. 2005; 71:5225–5235. [PubMed: 16151108]
8. White O, Eisen JA, Heidelberg JF, Hickey EK, Peterson JD, Dodson RJ, Haft DH, Gwinn ML, Nelson WC, Richardson DL, Moffat KS, Qin HY, Jiang LX, Pamphile W, Crosby M, Shen M, Vamathevan JJ, Lam P, McDonald L, Utterback T, Zalewski C, Makarova KS, Aravind L, Daly MJ, Minton KW, Fraser CM. Genome sequence of the radioresistant bacterium *Deinococcus radiodurans* R1. Science. 1999; 286:1571–1577. [PubMed: 10567266]
9. Tanaka M, Earl AM, Howell HA, Park MJ, Eisen JA, Peterson SN, Battista JR. Analysis of *Deinococcus radiodurans*'s transcriptional response to ionizing radiation and desiccation reveals novel proteins that contribute to extreme radioresistance. Genetics. 2004; 168:21–33. [PubMed: 15454524]
10. Gutsche I, Vujičić-Žagar A, Siebert X, Servant P, Vannier F, Castaing B, Heulin GBT, de Groot A, Sommer S, Serre L. Complex oligomeric structure of a truncated form of DdrA: A protein required for the extreme radiotolerance of *Deinococcus*. Biochim. Biophys. Acta (BBA) - Proteins & Proteomics. 2008; 1784:1050–1058.
11. Harris DR, Tanaka M, Saveliev SV, Jolivet E, Earl AM, Cox MM, Battista JR. Preserving Genome Integrity: The DdrA Protein of *Deinococcus radiodurans* R1. PLoS Biology. 2004; 2:e304. [PubMed: 15361932]
12. Harris DR, Ngo KV, Cox MM. The stable, functional core of DdrA from Deinococcus radiodurans R1 does not restore radioresistance in vivo. J. Bacteriol. 2008; 190:6475–6482. [PubMed: 18676665]
13. Norais CA, Chitteni-Pattu S, Wood EA, Inman RB, Cox MM. DdrB protein, an alternative *Deinococcus radiodurans* SSB induced by ionizing radiation. J. Biol. Chem. 2009; 284:21402–21411. [PubMed: 19515845]
14. Daly MJ, Gaidamakova EK, Matrosova VY, Vasilenko A, Zhai M, Leapman RD, Lai B, Ravel B, Li SM, Kemner KM, Fredrickson JK. Protein Oxidation Implicated as the Primary Determinant of Bacterial Radioresistance. PLoS Biol. 2007; 5:e92. [PubMed: 17373858]
15. Makarova KS, Omelchenko MV, Gaidamakova EK, Matrosova VY, Vasilenko A, Zhai M, Lapidus A, Copeland A, Kim E, Land M, Mavrommatis K, Pitluck S, Richardson PM, Detter C, Brettin T, Saunders E, Lai B, Ravel B, Kemner KM, Wolf YI, Sorokin A, Gerasimova AV, Gelfand MS, Fredrickson JK, Koonin EV, Daly MJ. *Deinococcus geothermalis*: the pool of extreme radiation resistance genes shrinks. PLoS One. 2007; 2:e955. [PubMed: 17895995]
16. Repar J, Cvjetan S, Slade D, Radman M, Zahradka D, Zahradka K. RecA protein assures fidelity of DNA repair and genome stability in *Deinococcus radiodurans* . DNA Repair. 2010; 9:1151–1161. [PubMed: 20817622]

17. Slade D, Lindner AB, Paul G, Radman M. Recombination and Replication in DNA Repair of Heavily Irradiated *Deinococcus radiodurans* . Cell. 2009; 136:1044–1055. [PubMed: 19303848]
18. Zahradka K, Slade D, Bailone A, Sommer S, Averbeck D, Petranovic M, Lindner AB, Radman M. Reassembly of shattered chromosomes in *Deinococcus radiodurans* . Nature. 2006; 443:569–573. [PubMed: 17006450]
19. Kim J-I, Cox MM. The RecA proteins of *Deinococcus radiodurans* and Escherichia coli promote DNA strand exchange via inverse pathways. Proc. Natl. Acad. Sci. U.S.A. 2002; 99:7917–7921. [PubMed: 12048253]
20. Hsu H-F, Ngo KV, Chitteni-Pattu S, Cox MM, Li H-W. Investigating *Deinococcus radiodurans* RecA protein filament formation on double-stranded DNA by a real-time single-molecule approach. Biochemistry. 2011; 50:8270–8280. [PubMed: 21853996]
21. Harris DR, Pollock SV, Wood EA, Goiffon RJ, Klingele AJ, Cabot EL, Schackwitz W, Martin J, Eggington J, Durfee TJ, Middle CM, Norton JE, Popelars M, Li H, Klugman SA, Hamilton LL, Bane LB, Pennacchio L, Albert TJ, Perna NT, Cox MM, Battista JR. Directed evolution of radiation resistance in *Escherichia coli* . J. Bacteriol. 2009; 191:5240–5252. [PubMed: 19502398]
22. Byrne RT, Klingele AJ, Cabot EL, Schackwitz WS, Martin JA, Martin J, Wang Z, Wood EA, Pennacchio C, Pennacchio LA, Perna NT, Battista JR, Cox MM. Evolution of extreme resistance to ionizing radiation via genetic adaptation of DNA Repair eLife. 2014; 3:e01322.
23. Haruta N, Yu XN, Yang SX, Egelman EH, Cox MM. A DNA pairing-enhanced conformation of bacterial RecA proteins. J. Biol. Chem. 2003; 278:52710–52723. [PubMed: 14530291]
24. Messing J. New M13 vectors for cloning. Methods Enzymol. 1983; 101:20–78. [PubMed: 6310323]
25. Neuendorf SK, Cox MM. Exchange of RecA protein between adjacent RecA protein-single-stranded DNA complexes. J. Biol. Chem. 1986; 261:8276–8282. [PubMed: 3755133]
26. Petrova V, Chitteni-Pattu S, Drees JC, Inman RB, Cox MM. An SOS Inhibitor that Binds to Free RecA Protein: The PsiB Protein. Mol. Cell. 2009; 36:121–130. [PubMed: 19818715]
27. Craig NL, Roberts JW. Function of nucleoside triphosphate and polynucleotide in *Escherichia coli* recA protein-directed cleavage of phage lambda repressor. J. Biol. Chem. 1981; 256:8039–8044. [PubMed: 6455420]
28. Lohman TM, Overman LB. Two binding modes in Escherichia coli single strand binding protein-single stranded DNA complexes. Modulation by NaCl concentration. J Biol. Chem. 1985; 260:3594–3603. [PubMed: 3882711]
29. Mertens N, Remaut E, Fiers W. Tight transcriptional control mechanism ensures stable high-level expression from T7 promoter-based expression plasmids. Biotechnology. 1995; 13:175–179. [PubMed: 9634760]
30. Lindsley JE, Cox MM. Assembly and disassembly of RecA protein filaments occurs at opposite filament ends: relationship to DNA strand exchange. J. Biol. Chem. 1990; 265:9043–9054. [PubMed: 2188972]
31. Morrical SW, Lee J, Cox MM. Continuous association of *Escherichia coli* single-stranded DNA binding protein with stable complexes of RecA protein and single-stranded DNA. Biochemistry. 1986; 25:1482–1494. [PubMed: 2939874]
32. Lusetti SL, Wood EA, Fleming CD, Modica MJ, Korth J, Abbott L, Dwyer DW, Roca AI, Inman RB, Cox MM. C-terminal deletions of the *Escherichia coli* RecA protein -Characterization of in vivo and in vitro effects. J. Biol. Chem. 2003; 278:16372–16380. [PubMed: 12598539]
33. Weinstock GM, McEntee K, Lehman IR. Hydrolysis of nucleoside triphosphates catalyzed by the recA protein of *Escherichia coli* Steady state kinetic analysis of ATP hydrolysis. J. Biol. Chem. 1981; 256:8845–8849. [PubMed: 6455429]
34. Brenner SL, Mitchell RS, Morrical SW, Neuendorf SK, Schutte BC, Cox MM. RecA protein-promoted ATP hydrolysis occurs throughout RecA nucleoprotein filaments. J. Biol. Chem. 1987; 262:4011–4016. [PubMed: 2951381]
35. Cox MM. Why Does RecA Protein Hydrolyze ATP. Trends Biochem Sci. 1994; 19:217–222. [PubMed: 8048163]
36. Cox JM, Tsodikov OV, Cox MM. Organized unidirectional waves of ATP hydrolysis within a RecA filament. PLoS Biology. 2005; 3:231–243.

37. Cox JM, Abbott SN, Chitteni-Pattu S, Inman RB, Cox MM. Complementation of one RecA protein point mutation by another - Evidence for trans catalysis of ATP hydrolysis. J. Biol. Chem. 2006; 281:12968–12975. [PubMed: 16527806]
38. Cox MM. Motoring along with the bacterial RecA protein. Nature Rev. Mol. Cell Biol. 2007; 8:127–138. [PubMed: 17228330]
39. Cox JM, Li H, Wood EA, Chitteni-Pattu S, Inman RB, Cox MM. Defective dissociation of a "Slow" RecA mutant protein imparts an *Escherichia coli* growth defect. J. Biol. Chem. 2008; 283:24909–24921. [PubMed: 18603529]
40. Cazaux C, Larminat F, Villani G, Johnson NP, Schnarr M, Defais M. Purification and biochemical characterization of *Escherichia coli* RecA proteins mutated in the putative DNA binding site. J. Biol. Chem. 1994; 269:8246–8254. [PubMed: 8132549]
41. Eggler AL, Lusetti SL, Cox MM. The C terminus of the *Escherichia coli* RecA protein modulates the DNA binding competition with single-stranded DNA-binding protein. J. Biol. Chem. 2003; 278:16389–16396. [PubMed: 12598538]
42. Lavery PE, Kowalczykowski SC. Biochemical basis of the constitutive repressor cleavage activity of recA730 protein A comparison to recA441 and recA803 proteins. J. Biol. Chem. 1992; 267:20648–20658. [PubMed: 1400384]
43. Mirshad JK, Kowalczykowski SC. Biochemical basis of the constitutive coprotease activity of RecA P67W protein. Biochemistry. 2003; 42:5937–5944. [PubMed: 12741852]
44. Schutte BC, Cox MM. Homology-dependent changes in adenosine 5'-triphosphate hydrolysis during RecA protein promoted DNA strand exchange: evidence for long paranemic complexes. Biochemistry. 1987; 26:5616–5625. [PubMed: 3314992]
45. Bedale WA, Cox M. Evidence for the coupling of ATP hydrolysis to the final (extension) phase of RecA protein-mediated DNA strand exchange. J. Biol. Chem. 1996; 271:5725–5732. [PubMed: 8621438]
46. Britt RL, Haruta N, Lusetti SL, Chitteni-Pattu S, Inman RB, Cox MM. Disassembly of Escherichia coli RecA E38K/ΔC17 Nucleoprotein Filaments Is Required to Complete DNA Strand Exchange. J. Biol. Chem. 2010; 285:3211–3226. [PubMed: 19910465]
47. Nayak S, Bryant FR. Differential rates of NTP hydrolysis by the mutant [S69G]RecA protein - Evidence for a coupling of NTP turnover to DNA strand exchange. J. Biol. Chem. 1999; 274:25979–25982. [PubMed: 10473540]
48. Joo C, McKinney SA, Nakamura M, Rasnik I, Myong S, Ha T. Real-time observation of RecA filament dynamics with single monomer resolution. Cell. 2006; 126:515–527. [PubMed: 16901785]
49. Lusetti SL, Hobbs MD, Stohl EA, Chitteni-Pattu S, Inman RB, Seifert HS, Cox MM. The RecF protein antagonizes RecX function via direct interaction. Mol. Cell. 2006; 21:41–50. [PubMed: 16387652]
50. Bell JC, Plank JL, Dombrowski CC, Kowalczykowski SC. Direct imaging of RecA nucleation and growth on single molecules of SSB-coated ssDNA. Nature. 2012; 491:274–U144. [PubMed: 23103864]
51. Galletto R, Amitani I, Baskin RJ, Kowalczykowski SC. Direct observation of individual RecA filaments assembling on single DNA molecules. Nature. 2006; 443:875–878. [PubMed: 16988658]
52. Cox MM, Goodman MF, Kreuzer KN, Sherratt DJ, Sandler SJ, Marians KJ. The importance of repairing stalled replication forks. Nature. 2000; 404:37–41. [PubMed: 10716434]
53. Cox MM. Historical overview: Searching for replication help in all of the rec places. Proc. Natl. Acad. Sci. U.S.A. 2001; 98:8173–8180. [PubMed: 11459950]
54. Chen ZC, Yang HJ, Pavletich NP. Mechanism of homologous recombination from the RecA-ssDNA/dsDNA structures. Nature. 2008; 453:489–494. [PubMed: 18497818]
55. Story RM, Weber IT, Steitz TA. The structure of the *E. coli* RecA protein monomer and polymer. Nature. 1992; 355:318–325. [PubMed: 1731246]
56. Wong OK, Guthold M, Erie DA, Gelles J. Interconvertible lac repressor-DNA loops revealed by single-molecule experiments. PloS Biol. 2008; 6:2028–2042.

57. Chu JF, Chang TC, Li HW. Single-Molecule TPM Studies on the Conversion of Human Telomeric DNA. Biophys. J. 2010; 98:1608–1616. [PubMed: 20409481]
58. Schafer DA, Gelles J, Sheetz MP, Landick R. Transcription by single molecules of RNA polymerase observed by light microscopy. Nature. 1991; 352:444–448. [PubMed: 1861724]
59. Dohoney KM, Gelles J. chi-Sequence recognition and DNA translocation by single RecBCD helicase/nuclease molecules. Nature. 2001; 409:370–374. [PubMed: 11201749]
60. Fan HF, Li HW. Studying RecBCD Helicase Translocation Along chi-DNA Using Tethered Particle Motion with a Stretching Force. Biophys. J. 2009; 96:1875–1883. [PubMed: 19254546]
61. Yin H, Landick R, Gelles J. Tethered particle motion method for studying transcription elongation by a single RNA polymerase molecule. Biophys J. 1994; 67:2468–2478. [PubMed: 7696485]
62. Pugh BF, Cox MM. Stable binding of RecA protein to duplex DNA Unraveling a paradox. J. Biol. Chem. 1987; 262:1326–1336. [PubMed: 3543002]
63. Pugh BF, Cox MM. General mechanism for RecA protein binding to duplex DNA. J. Mol. Biol. 1988; 203:479–493. [PubMed: 3058986]
64. Cox, MM. The RecA Protein. In: Higgins, NP., editor. The Bacterial Chromosome. Washington, D. C: American Society of Microbiology; 2004. p. 369-388.
65. Cox, MM. The bacterial RecA protein: structure, function, and regulation. In: Rothstein, R.; Aguilera, A., editors. Topics in Current Genetics: Molecular Genetics of Recombination. Heidelberg: Springer-Verlag; 2007. p. 53-94.
66. Lusetti SL, Cox MM. The bacterial RecA protein and the recombinational DNA repair of stalled replication forks. Annu. Rev. Biochem. 2002; 71:71–100. [PubMed: 12045091]
67. Cox MM, Soltis DA, Lehman IR, DeBrosse C, Benkovic SJ. ADP-mediated dissociation of stable complexes of RecA protein and single-stranded DNA. J. Biol. Chem. 1983; 258:2586–2592. [PubMed: 6337158]
68. Lee JW, Cox MM. Inhibition of RecA protein-promoted ATP hydrolysis. I. ATPγS and ADP are antagonistic inhibitors. Biochemistry. 1990; 29:7666–7676. [PubMed: 2148682]
69. Lee JW, Cox MM. Inhibition of RecA protein-promoted ATP hydrolysis. II. Longitudinal assembly and disassembly of RecA protein filaments mediated by ATP and ADP. Biochemistry. 1990; 29:7677–7683. [PubMed: 2271526]
70. Buckstein MH, He J, Rubin H. Characterization of nucleotide pools as a function of physiological state in *Escherichia coli* . J. Bacteriol. 2008; 190:718–726. [PubMed: 17965154]
71. Little JW. Mechanism of specific LexA cleavage - autodigestion and the role of RecA coprotease. Biochimie. 1991; 73:411–422. [PubMed: 1911941]
72. Rehrauer WM, Lavery PE, Palmer EL, Singh RN, Kowalczykowski SC. Interaction of *Escherichia coli* RecA protein with LexA repressor. 1 LexA repressor cleavage is competitive with binding of a secondary DNA molecule. J. Biol. Chem. 1996; 271:23865–23873. [PubMed: 8798617]
73. Yu X, Egelman EH. The LexA repressor binds within the deep helical groove of the activated RecA filament. J. Mol. Biol. 1993; 231:29–40. [PubMed: 8496964]
74. Drees JC, Lusetti SL, Chitteni-Pattu S, Inman RB, Cox MM. A RecA filament capping mechanism for RecX protein. Mol. Cell. 2004; 15:789–798. [PubMed: 15350222]
75. Gruenig MC, Stohl EA, Chitteni-Pattu S, Seifert HS, Cox MM. Less Is More: *Neisseria gonorrhoeae* RecX Protein Stimulates Recombination by Inhibiting RecA. J. Biol. Chem. 2010; 285:37188–37197. [PubMed: 20851893]
76. Stohl EA, Brockman JP, Burkle KL, Morimatsu K, Kowalczykowski SC, Siefert HS. *Escherichia coli* RecX inhibits RecA recombinase and coprotease activities in vitro and in vivo. J. Biol. Chem. 2003; 278:2278–2285. [PubMed: 12427742]
77. Jiang Q, Karata K, Woodgate R, Cox MM, Goodman MF. The active form of DNA polymerase V is UmuD'2C•RecA•ATP. Nature. 2009; 460:359–363. [PubMed: 19606142]
78. Patel M, Jiang QF, Woodgate R, Cox MM, Goodman MF. A new model for SOS-induced mutagenesis: how RecA protein activates DNA polymerase V. Crit. Rev. Biochem. Mol. Biol. 2010; 45:171–184. [PubMed: 20441441]
79. Schlacher K, Cox MM, Woodgate R, Goodman MF. RecA acts in trans to allow replication of damaged DNA by DNA polymerase V. Nature. 2006; 442:883–887. [PubMed: 16929290]

80. Ngo KV, Molzberger ET, Chitteni-Pattu S, Cox MM. Regulation of *Deinococcus radiodurans* RecA protein function via modulation of active and inactive nucleoprotein filament states. J. Biol. Chem. 2013; 288:21351–21366. [PubMed: 23729671]
81. Story RM, Steitz TA. Structure of the RecA Protein-ADP complex. Nature. 1992; 355:374–376. [PubMed: 1731253]
82. Roca AI, Cox MM. The RecA protein: structure and function. CRC Crit. Rev. Biochem. Mol. Biol. 1990; 25:415–456. [PubMed: 2292186]
83. Kurumizaka H, Aihara H, Ikawa S, Kashima T, Bazemore LR, Kawasaki K, Sarai A, Radding CM, Shibata T. A possible role of the C-terminal domain of the RecA protein A gateway model for double-stranded DNA binding. J. Biol. Chem. 1996; 271:33515–33524. [PubMed: 8969216]
84. Stohl EA, Gruenig MC, Cox MM, Seifert HS. Purification and Characterization of the RecA Protein from *Neisseria gonorrhoeae* . Plos One. 2011; 6
85. Angov E, Camerini OR. The recA gene from the thermophile *Thermus aquaticus* YT-1: cloning, expression, and characterization. J. Bacteriol. 1994; 176:1405–1012. [PubMed: 8113181]
86. Pierré A, Paoletti C. Purification and characterization of a RecA protein from *Salmonella typhimurium* . J. Biol. Chem. 1983; 258:2870–2874. [PubMed: 6219107]
87. Ganesh N, Muniyappa K. Characterization of DNA strand transfer promoted by *Mycobacterium smegmatis* RecA reveals functional diversity with *Mycobacterium tuberculosis* RecA. Biochemistry. 2003; 42:7216–7225. [PubMed: 12795618]
88. Bakhlanova IV, Dudkina AV, Baitin DM, Knight KL, Cox MM, Lanzov VA. Modulating cellular recombination potential through alterations in RecA structure and regulation. Mol. Microbiol. 2010; 78:1523–1538. [PubMed: 21143322]

Highlights

- Mutations in the *recA* gene at position 276 confer resistance to gamma irradiation.
- The mutant proteins work efficiently when sub-stoichiometric relative to DNA.
- The mutant proteins are less inhibited by ADP.

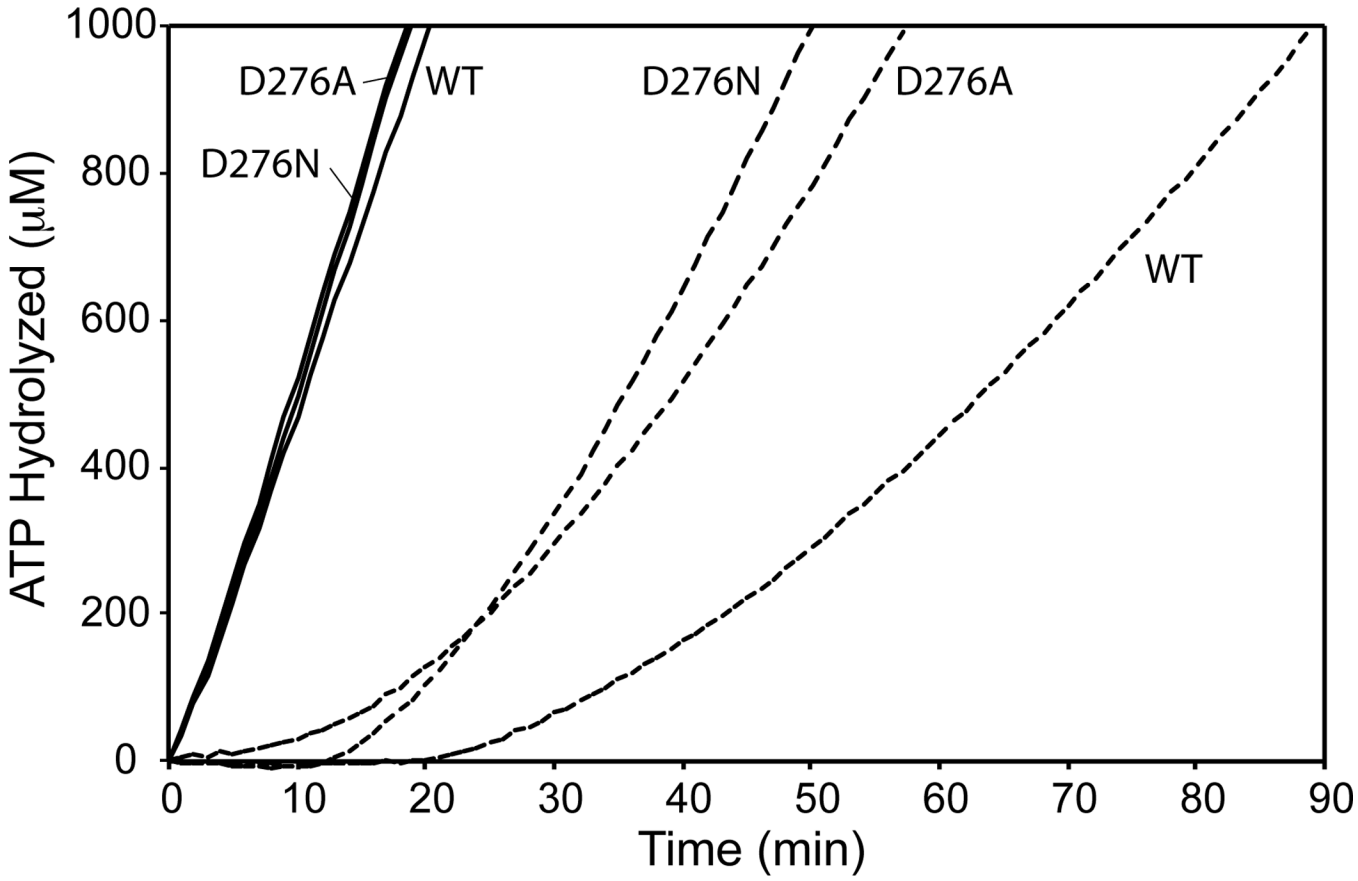

Fig. 1.

RecA D276A and RecA D276N hydrolyze ATP faster when bound to circular ssDNA and more readily displace the SSB protein from circular ssDNA than Wild type RecA. The DNA-dependent RecA-catalyzed hydrolysis of ATP was monitored. Reactions were carried out as described in *Experimental Procedures*. Solid lines represent reactions in which RecA protein was added first to a solution containing circular ssDNA, and dashed lines represent reactions in which SSB and ATP were added first to circular ssDNA. The 0 time point corresponds to either the time of addition of ATP and SSB (solid lines) or the addition of RecA protein (dashed lines).

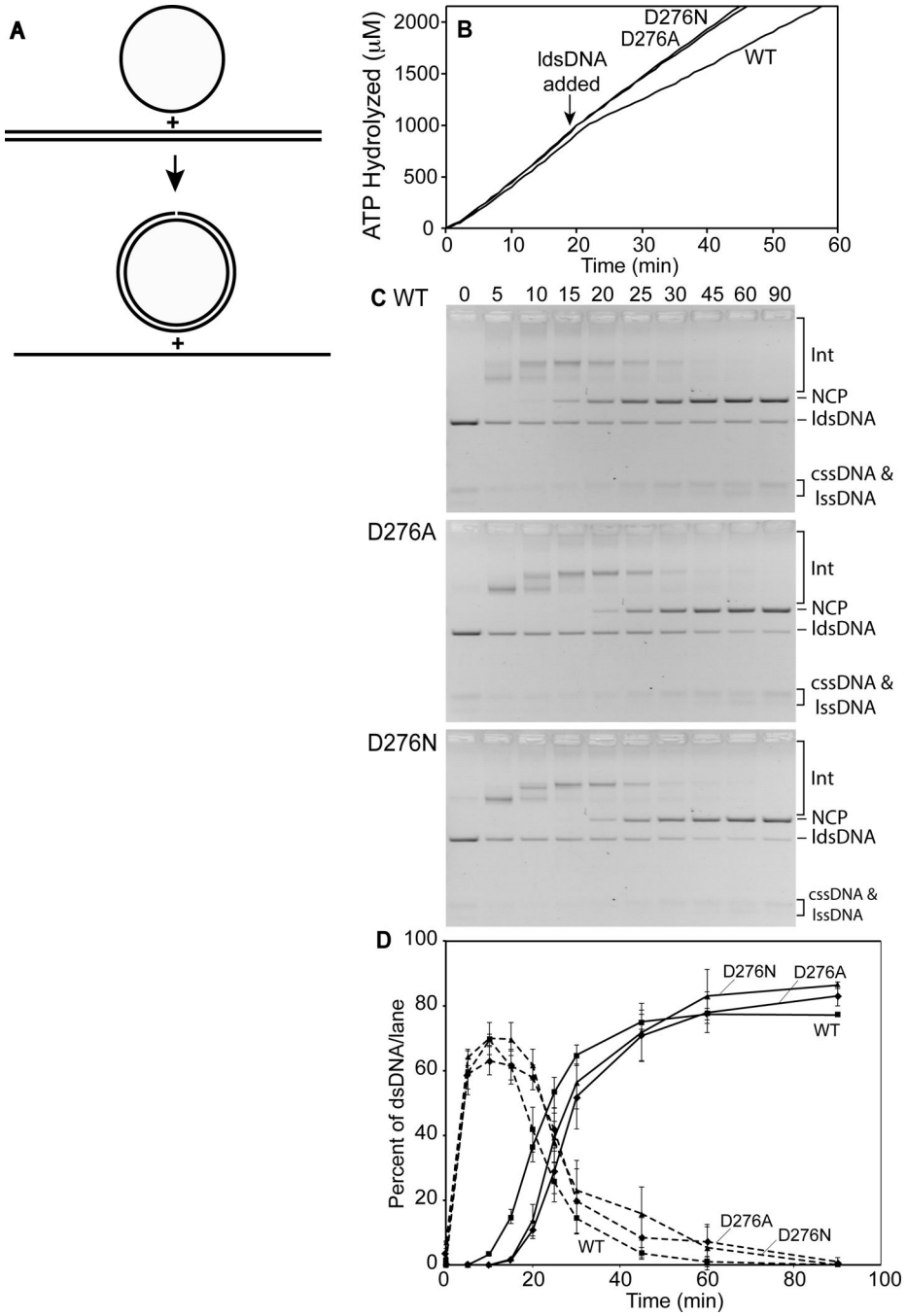

Fig. 2.

RecA D276A and RecA D276N hydrolyze ATP faster while catalyzing strand exchange but resolve strand exchange intermediates into products slower than Wild type RecA. *A*, The DNA strand exchange reaction promoted by RecA protein. *B.* ATP hydrolysis was monitored. Reactions were carried out as described in *Experimental Procedures*. First, 3 μM RecA protein was added to 5 μM M13mp18 circular ssDNA and incubated for 10 minutes. Then, ATP hydrolysis was initiated by the addition of 3 mM ATP and 0.5 μM SSB. Strand exchange reactions were initiated 20 min later by the addition of 10 μM homologous

M13mp18 linear dsDNA (time marked with an arrow). Time 0 corresponds to the time of addition of ATP and SSB. *C*, Agarose gel pictures displaying the progression of the strand exchange reactions. DNA bands are labeled as seen in the reaction schematic. Time 0 corresponds to the addition of linear dsDNA to the reactions. *D*, The amount of nicked circular product DNA was quantified at each time point as the percentage of the total intenstity of linear dsDNA, intermediates, and product DNA in the corresponding lane. Wild type RecA reaction points are shown as squares, RecA D276A reaction points are shown as diamonds, and RecA D276N reaction points are shown as triangles. Values represent the averages of three independent experiments, with vertical error bars displaying the standard deviation of these values.

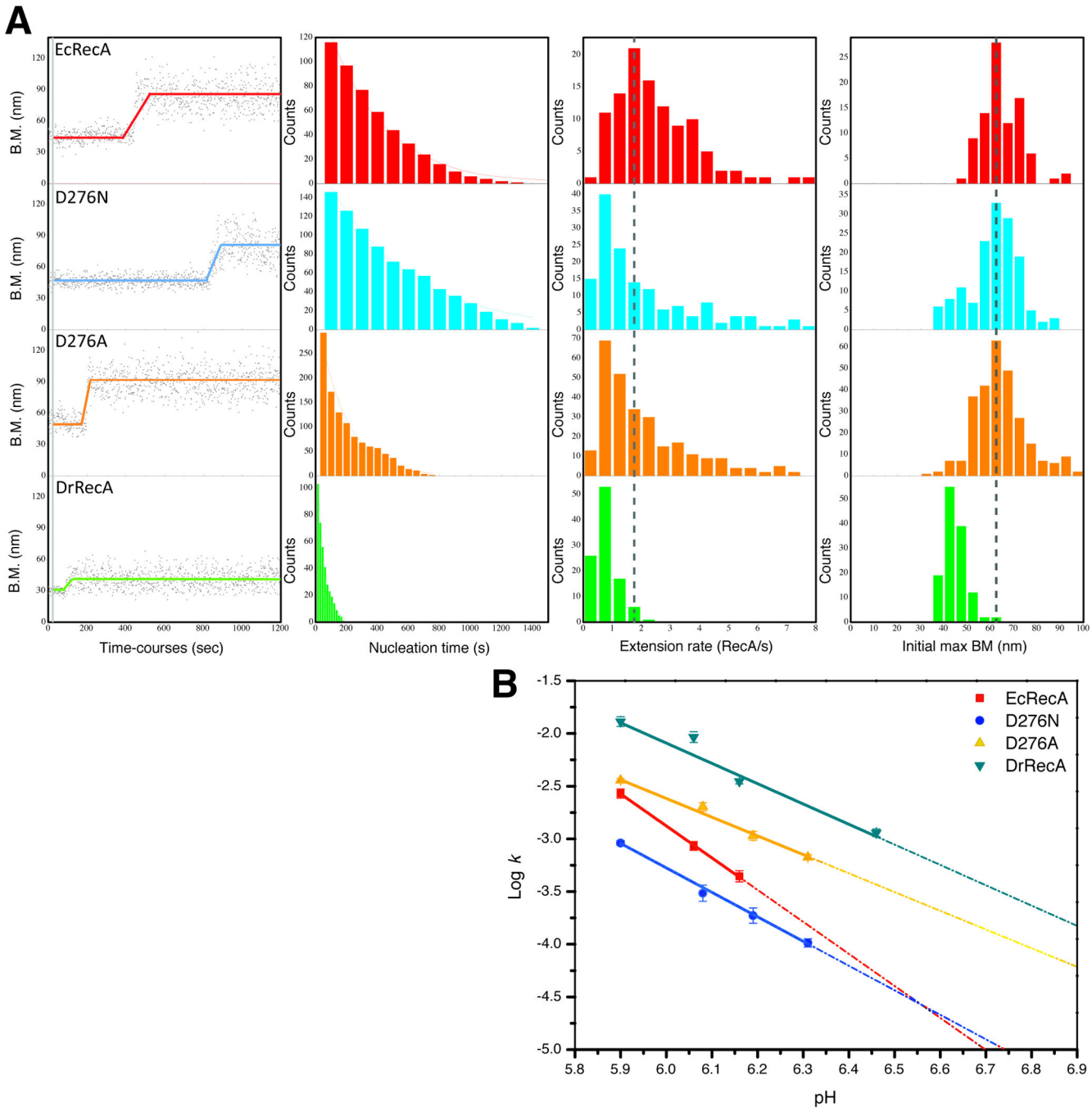

Fig. 3.

Single-molecule TPM observation of the nucleoprotein filament assembly process of EcRecA, D276N mutant, D276A mutant and DrRecA on dsDNA. (A). Exemplary time-courses of the filament assembly process on 382 bp dsDNA at pH 6.20. The RecA mixture was flowed in during the time represented by the short vertical gray bar at the beginning of each reacion. Before RecA forms a stable nucleus, the BM amplitude stays constant, the same as that before the gray bar. A stable nucleus is followed by a cooperative extension process, which is represented by the continuous BM increase. After the filament assembly is

finished, the BM amplitude reaches a maximum plateau value. In the subsequent three columns are the accumulated histograms of observed nucleation times (the point in each trial in which BM begins to increase), observed extension rates, and observed maximum BM amplitudes. The histograms include 116, 146, 293, and 103 individual observed filaments of EcRecA, D276N, D276A and DrRecA, respectively. (B) pH-rate profiles for the measured nucleation rates for the proteins listed.

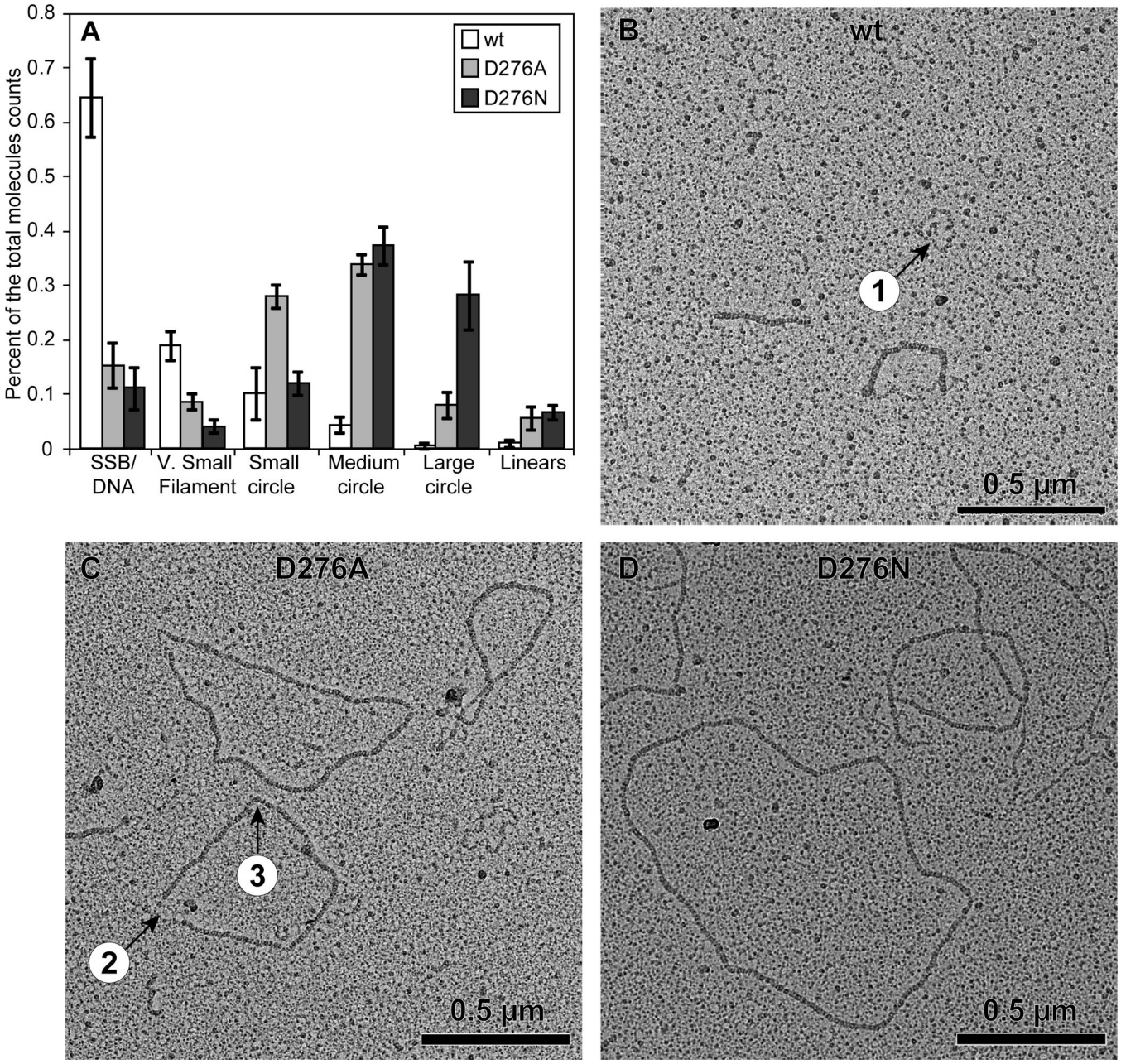

Fig. 4.

Early stages of filament formation by RecA wild type and variants on SSB-coated ssDNA. RecA protein filaments were spread and visualized as described in methods. *A*. Summary of filament categories present 5 min after RecA addition to ssDNA. Representative images are shown in panels *B, C*, and *D*. Molecule highlighted as #1 in panel *B* is an SSB-coated ssDNA circle. A visible gap (2) and a sharp filament bend are highlighted in panel *C*.

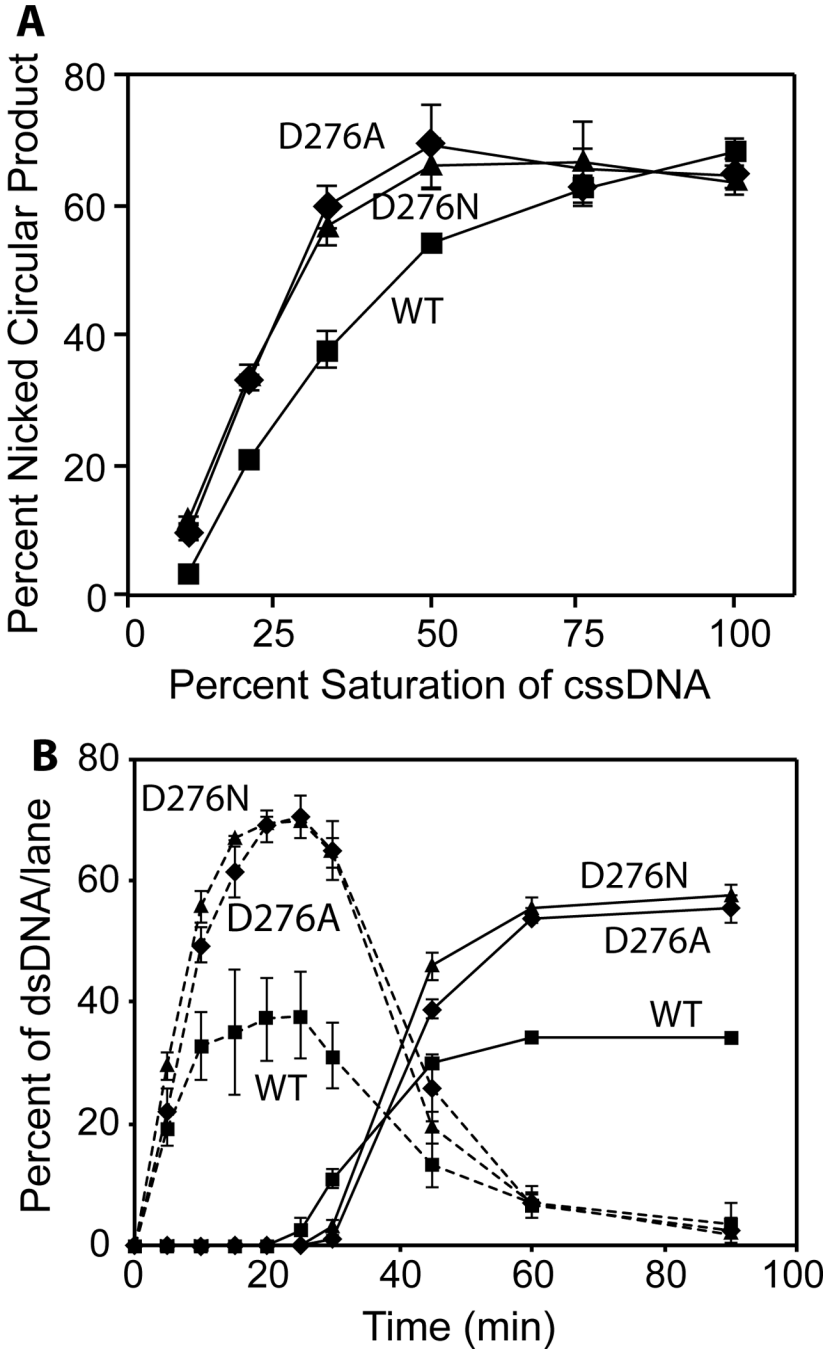

Fig. 5.

RecA D276A and RecA D276N more efficiently catalyze strand exchange reactions than Wild type RecA when present at sub-saturating levels of circular ssDNA. *A*, Strand exchange reactions were carried out as described in *Experimental Procedures* with RecA protein present at 10%, 20%, 33%, 50%, 75%, and 100% saturation of circular ssDNA. Reactions were deproteinized 90 minutes after the addition of linear dsDNA, resolved on an agarose gel, and the amount of circular duplex product DNA was quantified as described in Figure 2. Symbols are: ▪, wild type RecA; ♦, RecA D276A; and ▲, RecA D276N. Values of

percent nicked circular product represent the averages of three independent experiments, with vertical error bars displaying the standard deviation of these values. Reactions contained varying amounts of RecA protein, 10 μM M13mp18 circular ssDNA, 20 μM M13mp18 linear dsDNA, 3 mM ATP, and 1 μM SSB. *B*, The amount of intermediates or product DNA at each time point from a strand exchange time course in which each RecA protein is present at 33% saturation of the circular ssDNA, quantified as described in Figure 2. Symbols are as in panel A. Points connected with a dashed line display the amount of reaction intermediates present at each time point, while points connected with a solid line display the amount of product DNA present at each time point. Values displayed represent the averages of three independent experiments, with vertical error bars displaying the standard deviation of these values.

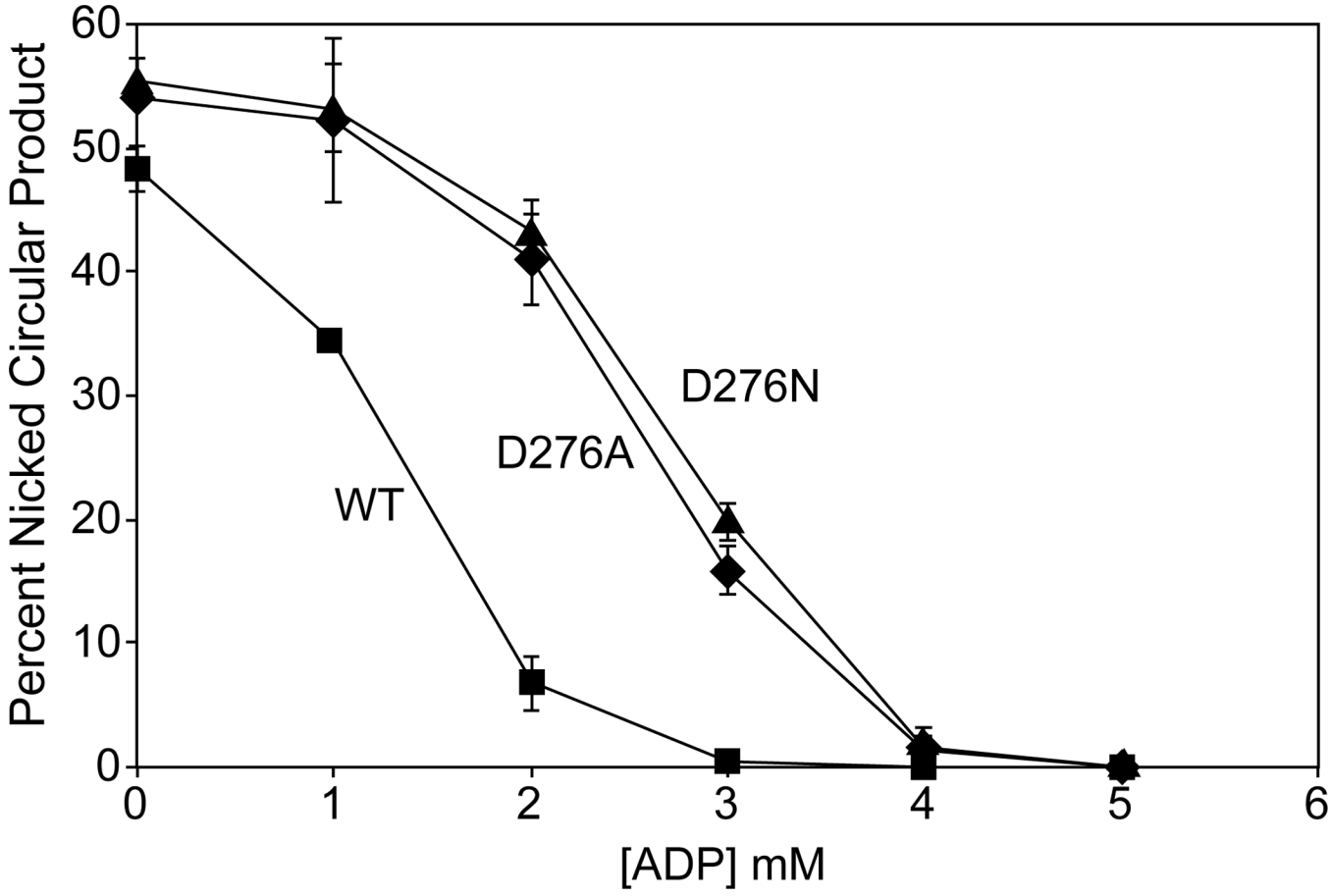

Fig. 6.

The strand exchange activitity of RecA D276A and RecA D276N is less inhibited by ADP than that of Wild type RecA. Strand exchange reactions were carried out as described in *Experimental Procedures*, with varying concentrations of ADP. Reactions contained 5 μM M13mp18 circular ssDNA, 2 μM RecA protein (100% saturation of the available ssDNA), 5 mM ATP, and 0.5 μM SSB. To initiate strand exchange, 10 μM M13mp18 linear dsDNA was added to the reactions with 0, 1, 2, 3, 4, or 5 mM ADP. Reactions were deproteinized 60 minutes after the addition of linear dsDNA, resolved on an agarose gel, and the amount of product DNA was quantified as described in Figure 2. Values displayed on the graph are averages of data from three independent experiments, and vertical error bars represent the standard deviation of these values. Wild type RecA points are shown as squares, RecA D276A points are shown as diamonds, and RecA D276N points are shown as triangles.

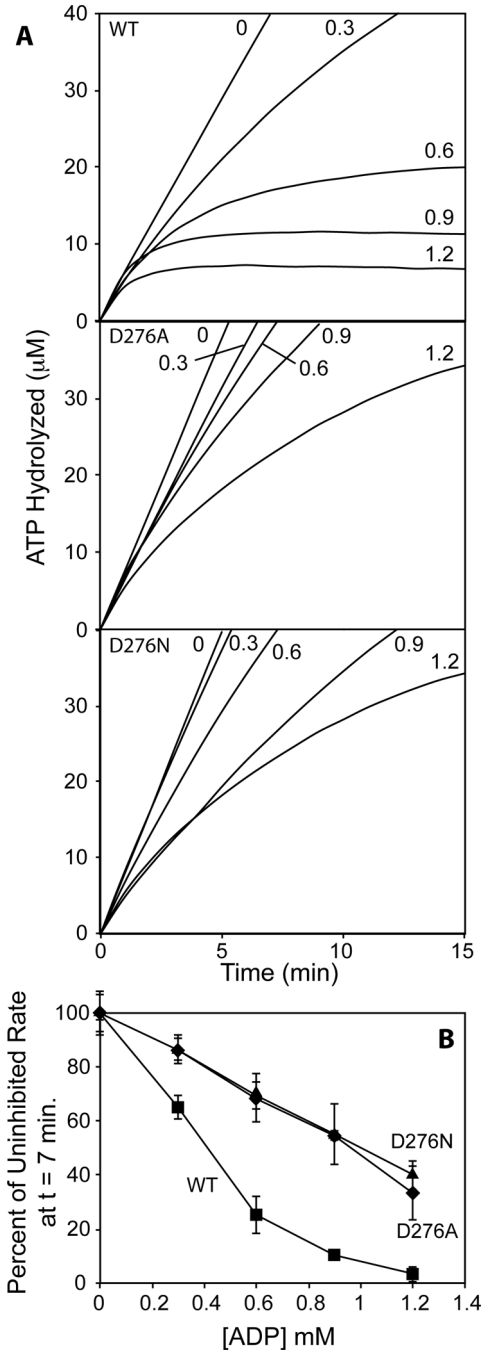

Fig. 7.

The ATPase activity of RecA D276A and RecA D276N during strand exchange is less inhibited by ADP than that of Wild type RecA. *A*, Reactions were carried out as described in *Experimental Procedures*, and ATP hydrolysis was monitored. First, 0.6 μM RecA protein was allowed to hydrolyze ATP in the presence of 1 μM M13mp18 circular ssDNA, 1.5 mM ATP, and 0.1 μM SSB for five minutes, and then 2 μM homologous M13mp18 linear dsDNA and 0, 0.3, 0.6, 0.9, 1.2, or 1.5 mM ADP were added as a mixture. Graphs are labeled with the variant of RecA protein used in the reactions, and reaction lines are labeled

with the concentration of ADP added. Time 0 corresponds to the addition of linear dsDNA and ADP. *B,* ATP hydrolysis data was fit with a polynomial curve and this fit was differentiated at time 7 minutes after the addition of linear dsDNA and ADP to determine the rate of hydrolysis of ATP at that time. Values from three independent experiments were averaged, and then expressed as the percentage of the rate at 7 minutes in the reaction in which no ADP was added. Vertical error bars display propogated standard deviation. Wild type RecA points are shown as squares, RecA D276A points are shown as diamonds, and RecA D276N points are shown as triangles

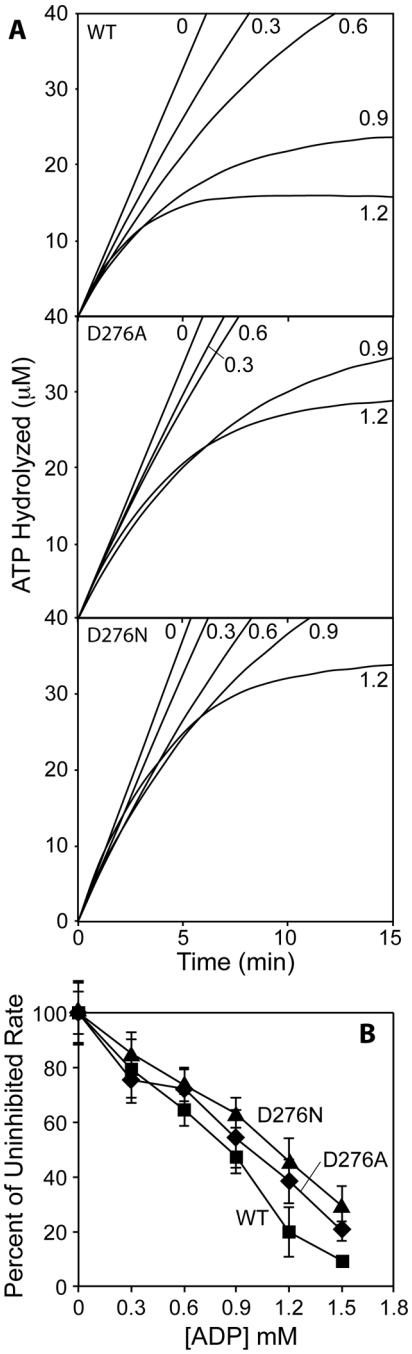

Fig. 8.

The ATPase activity of RecA D276A and RecA D276N on circular ssDNA is only slightly less inhibited by ADP than that of Wild type RecA. *A*, reactions were carried out as in Figure 6 but without homologous linear dsDNA, and ATP hydrolysis was monitored. Graphs are labeled with the variant of RecA protein used in the reactions, and reaction lines are labeled with the concentration of ADP added. Time 0 corresponds to the addition of ADP. *B*, The rate of ATP hydrolysis at time 7 minutes after the addition of ADP was quantified and converted to percentage of the rate of the reaction to which no ADP was

added as described in Figure 6. Wild type RecA points are shown as squares, RecA D276A points are shown as diamonds, and RecA D276N points are shown as triangles.